QCD at Small *x* and Saturation

Yuri Kovchegov
The Ohio State University

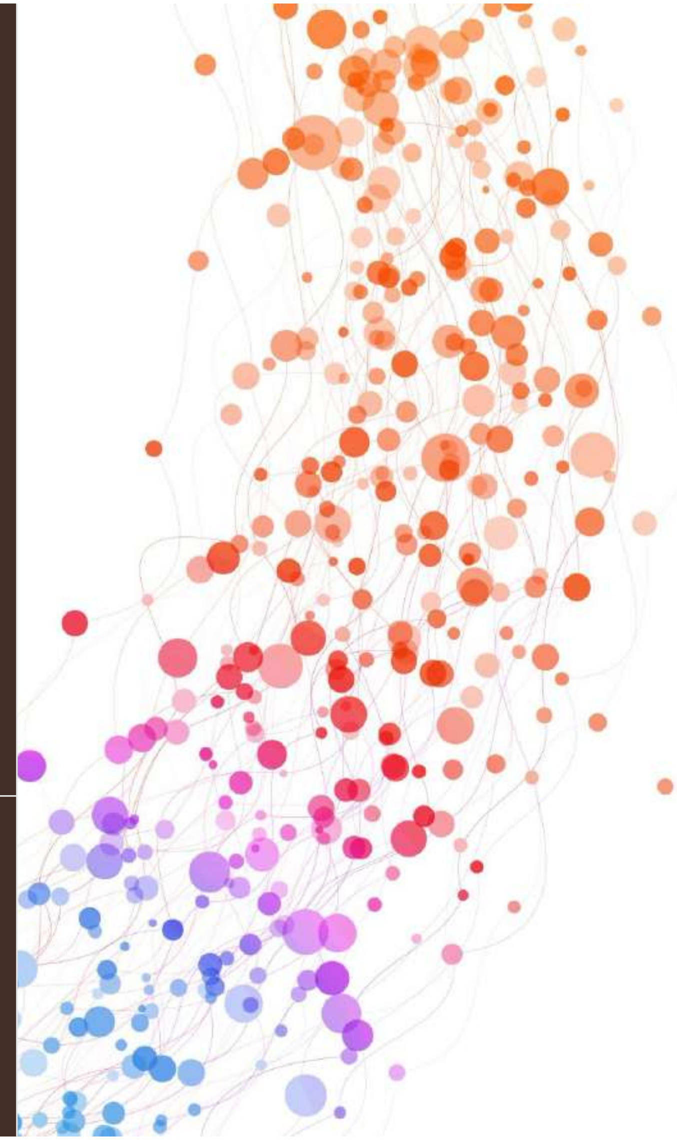

Lecture plan

- General concepts of saturation physics
- DIS: a brief reminder.
- Classical small-*x* physics:
  - DIS in the dipole picture, light-cone perturbation theory, light-cone wave functions
  - Glauber-Gribov-Mueller formula
  - Black disk limit, parton saturation, saturation scale
  - McLerran-Venugopalan model, saturation scale for a nucleus
- Nonlinear small-*x* evolution:
  - Non-linear BK and JIMWLK evolution equations
  - Solution of BK and JIMWLK equations, unitarity,
    energy dependence of the saturation scale, geometric scaling
- Saturation physics at the future EIC

General Concepts

Big goal: understand QCD at high energies.
What is the high-energy asymptotic behavior of QCD?

Running of QCD Coupling Constant

⇨QCD coupling constant $\alpha_S = \frac{g^2}{4\pi}$ changes with the momentum scale involved in the interaction

$$\alpha_S = \alpha_S(Q)$$

Asymptotic Freedom!

Gross and Wilczek, Politzer, ca '73

Physics Nobel Prize 2004!

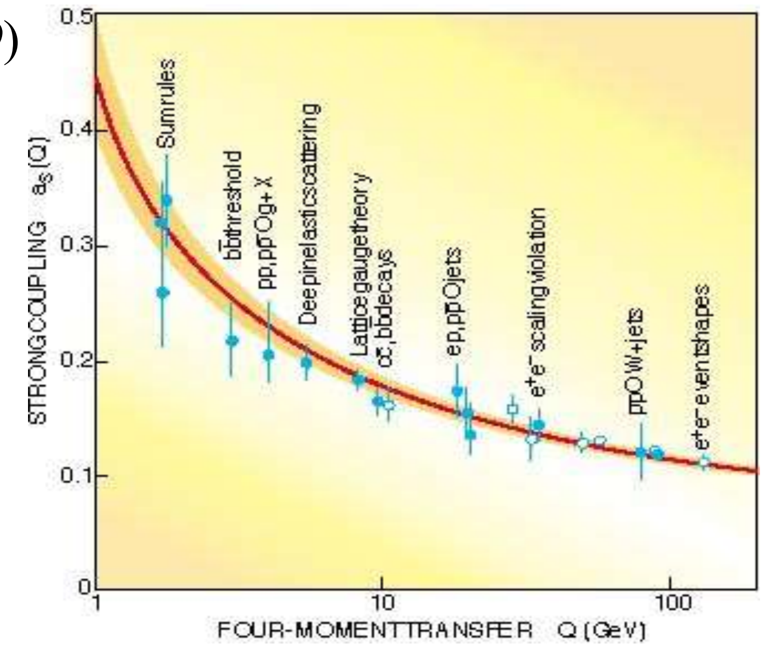

For short distances x < 0.2 fm, or, equivalently, large momenta k > 1 GeV the QCD coupling is small, $\alpha_S << 1$ and interactions are weak.

What sets the scale of running QCD coupling in high energy collisions?

- "Optimist": $$\alpha_S = \alpha_S\left(\sqrt{s}\right) << 1$$
- Pessimist: $\alpha_S = \alpha_S\left(\Lambda_{QCD}\right) \sim 1$ we simply can not tackle high energy scattering in QCD.
- pQCD: only study high-p_T particles such that

$$\alpha_S = \alpha_S\left(p_T\right) << 1$$

But: what about total cross section? bulk of particles?

What sets the scale of running QCD coupling in high energy collisions?

- Saturation physics is based on the existence of a large internal momentum scale Q_S which grows with both energy s and nuclear atomic number A

$$Q_S^2 \sim A^{1/3}\ s^{\lambda}$$

such that

$$\alpha_S = \alpha_S(Q_S) << 1$$

and we can calculate total cross sections, particle spectra and multiplicities, etc, from <u>first principles</u>.

The main principle

- Saturation physics is based on the existence of a large internal transverse momentum scale Q_S which grows with both decreasing Bjorken *x* and with increasing nuclear atomic number A

$$Q_s^2 \sim A^{1/3} \left(\frac{1}{x}\right)^{\lambda}$$

such that

$$\alpha_S = \alpha_S(Q_S) << 1$$

and we can use perturbation theory to calculate total cross sections, particle spectra and multiplicities, correlations, etc, from first principles.

Quasi-classical approximation

A. Glauber-Mueller Rescatterings

Kinematics of DIS

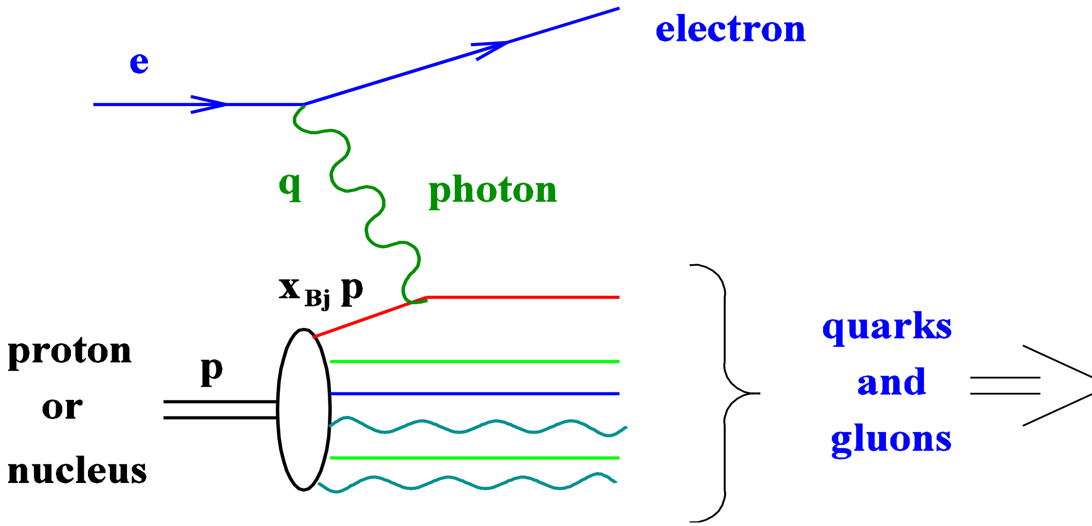

- Photon carries 4-momentum q_μ , its virtuality is

$$Q^2 = -q_\mu \, q^\mu$$

- Photon hits a quark in the proton carrying momentum $x_{Bj} p$ with p being the proton's momentum. Parameter x_{Bj} is the Bjorken *x* variable.

Physical Meaning of Q

Uncertainty principle teaches us that

$$\Delta p \Delta l \approx \hbar$$

which means that the photon probes the proton at the distances of the order (ħ=1)

$$\Delta l \sim \frac{1}{Q}$$

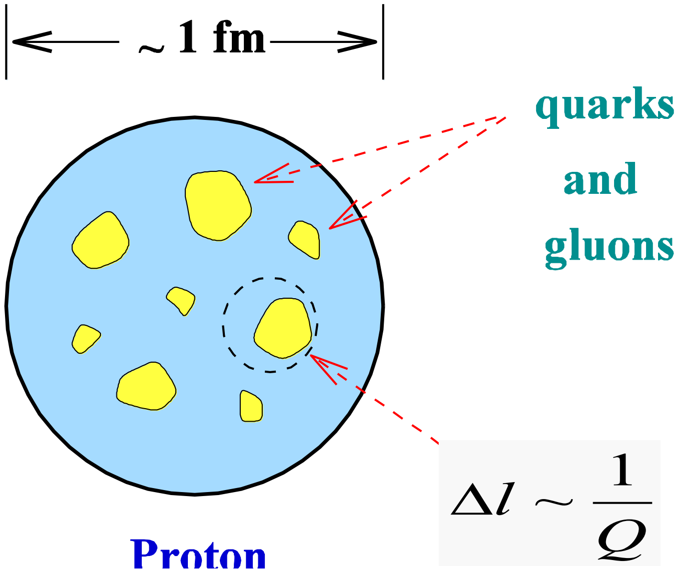

Large Momentum Q = Short Distances Probed

Physical Meaning of Bjorken *x*

The quarks and gluons that interact with the target have their typical momenta on the order of the typical momentum in the target,

$$x_{Bj}\, p \;\approx q \approx m.$$

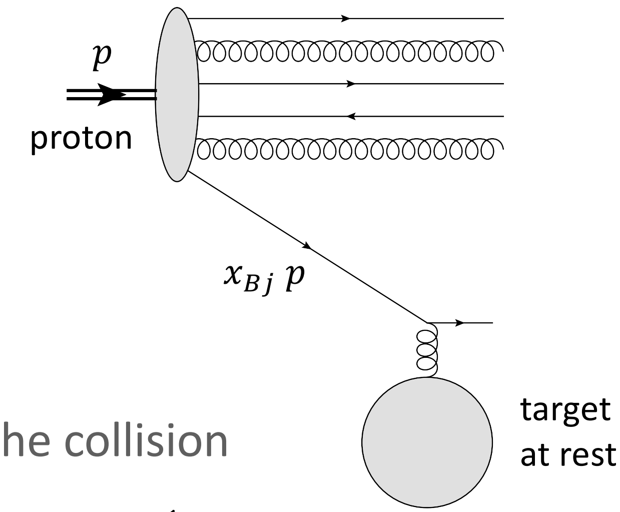

Then the energy of the collision

$$E \sim p \sim \frac{1}{x_{Bj}}$$

High Energy = Small *x*

Gluons at Small *x*

- There is a large number of small-*x* gluons (and quarks) in a proton:

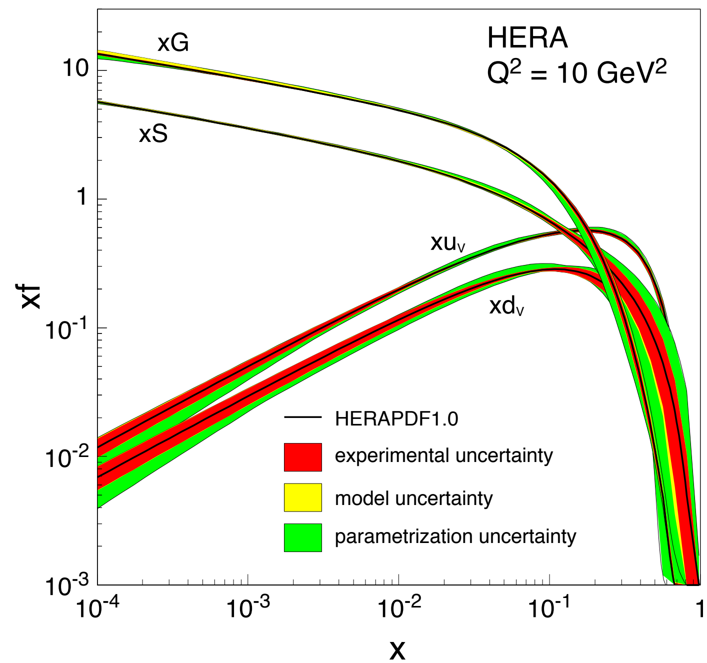

- *$G(x, Q^2)$, $q(x, Q^2)$* = gluon and quark number densities (q=u,d, or S for sea).

Gluons and Quarks in the Proton

⇨ There is a huge number of quarks, anti-quarks and gluons at small-x !

⇨ How do we reconcile this result with the picture of the proton made up of three valence quarks?

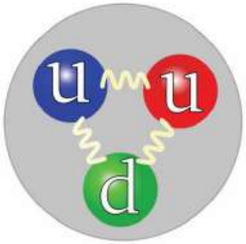

⇨ Qualitatively we understand that these extra quarks and gluons are emitted by the original three valence quarks in the proton.

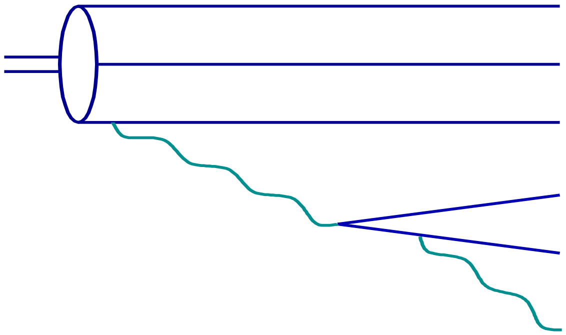

Dipole picture of DIS

$$W^{\mu\nu} = \frac{1}{4\pi M_p} \int d^4x \, e^{iq\cdot x} \langle P | j^\mu(x) \, j^\nu(0) | P \rangle$$

$$q^\mu = \left(\frac{Q^2}{2q^-}, q^-, 0_\perp \right)$$

Large q^- → large x^- separation

$$e^{iq\cdot x} = e^{i\frac{Q^2}{2q^-}x^- + iq^- x^+}$$

$$x^\pm = \frac{t \pm z}{\sqrt{2}}$$

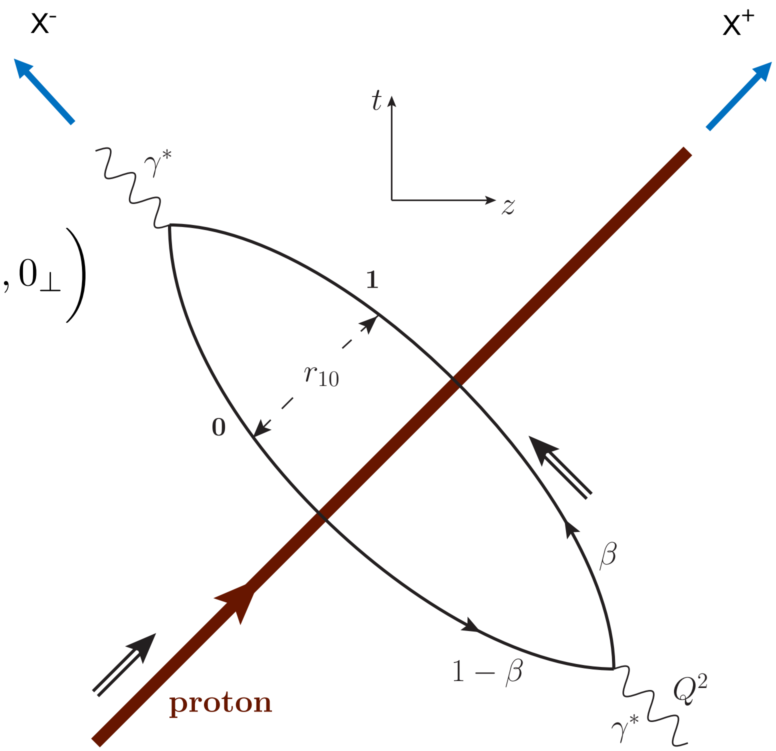

aka the "shock wave"

Dipole picture of DIS

- At small x, the dominant contribution to DIS structure functions does not come from the handbag diagram.

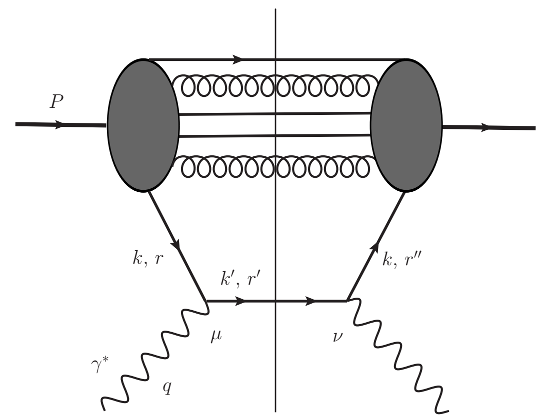

- Instead, the dominant terms comes from the dipole picture of DIS, where the virtual photon splits into a quark-antiquark pair, which then interacts with the target.

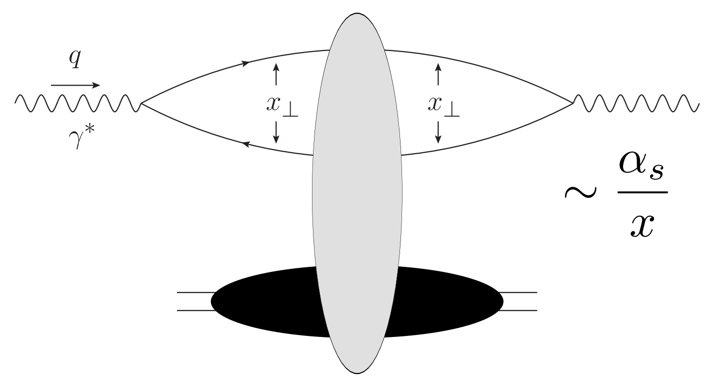

$$\sim \frac{\alpha_s}{x}$$

Dipole Amplitude

- The total DIS cross section is expressed in terms of the (Im part of the) forward quark dipole amplitude N:

$$\sigma_{tot}^{\gamma^* A} = \int \frac{d^2 x_\perp}{2\,\pi}\, d^2 b_\perp \int\limits_0^1 \frac{dz}{z\,(1-z)}\; |\Psi^{\gamma^* \to q\bar{q}}(\vec{x}_\perp, z)|^2 \; N(\vec{x}_\perp, \vec{b}_\perp, Y)$$

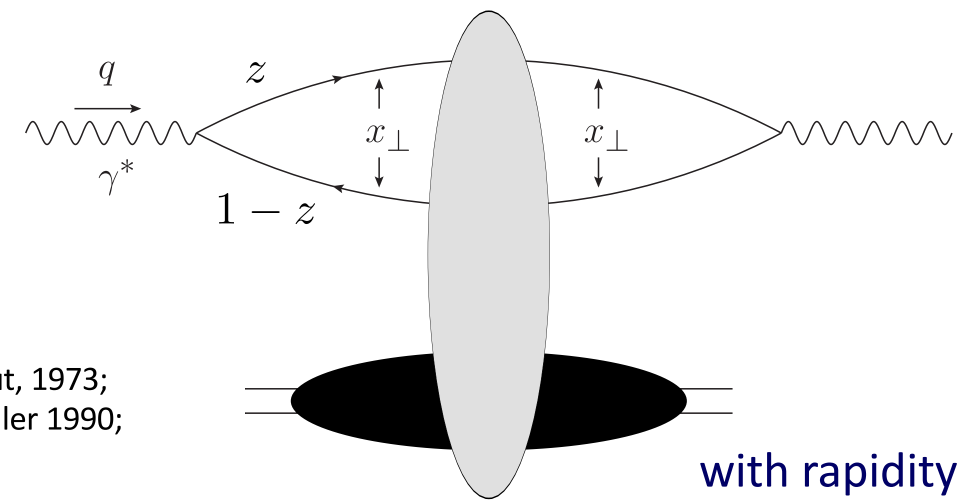

b is the Fourier conjugate to q with t = - q^2, making the dipole amplitude N similar to the GPDs at zero skewness.

$b_\perp, \; Y$

Gribov, 1970; Bjorken and Kogut, 1973; Frankfurt, Strikman 1988; Mueller 1990; Nikolaev and Zakharov 1991

with rapidity Y=ln(1/x)

DIS in the Classical Approximation

The DIS process in the rest frame of the target nucleus is shown below.

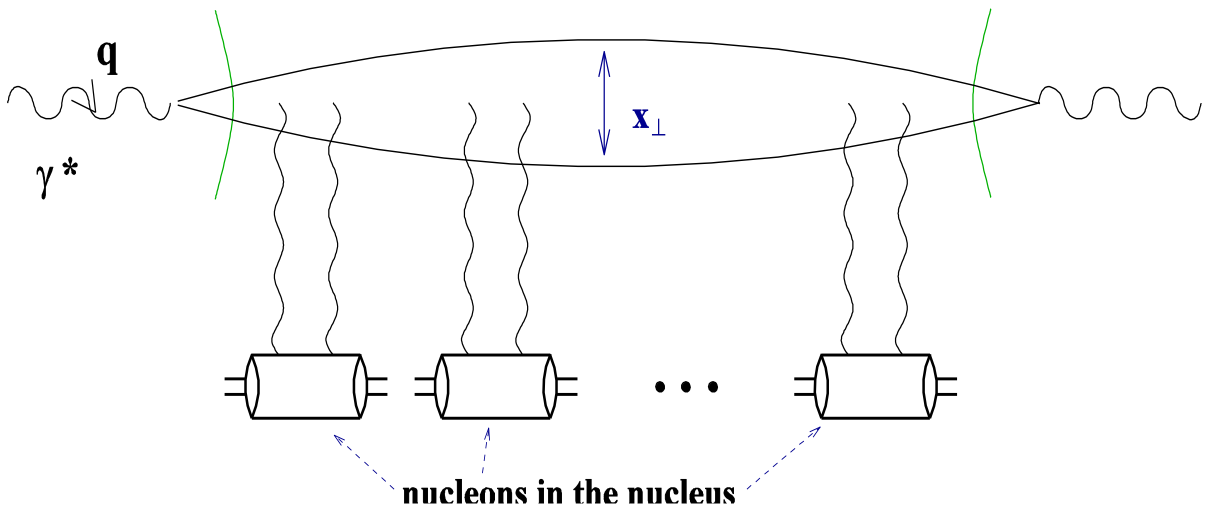

$$\sigma_{tot}^{\gamma * A}(x_{Bj}, Q^2) = |\Psi^{\gamma * \to q\bar{q}}|^2 \otimes N(x_\perp, Y = \ln 1/x_{Bj})$$

with rapidity Y=ln(1/x)

Dipole Amplitude

- The quark dipole amplitude is defined by

$$N(\underline{x}_1, \underline{x}_2) = 1 - \frac{1}{N_c} \left\langle \text{tr} \left[V(\underline{x}_1) \, V^\dagger(\underline{x}_2) \right] \right\rangle$$

- Here we use the Wilson lines along the light-cone direction

$$V_{\underline{x}} = \mathcal{P} \exp \left[ig \int\limits_{-\infty}^{\infty} dx^- A^+(0^+, x^-, \underline{x}) \right]$$

- In the classical Glauber-Mueller/McLerran-Venugopalan approach the dipole amplitude resums multiple rescatterings:

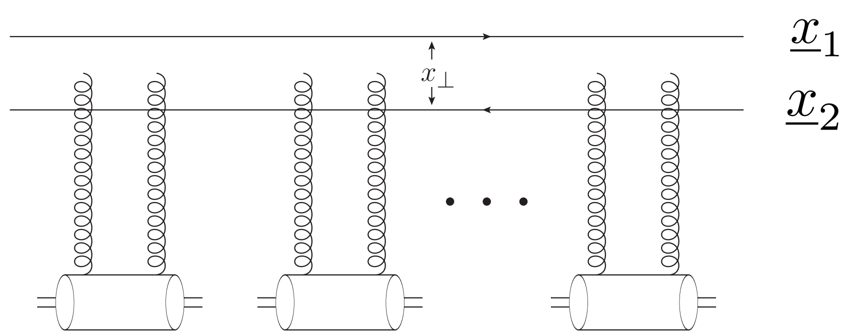

Quasi-classical dipole amplitude

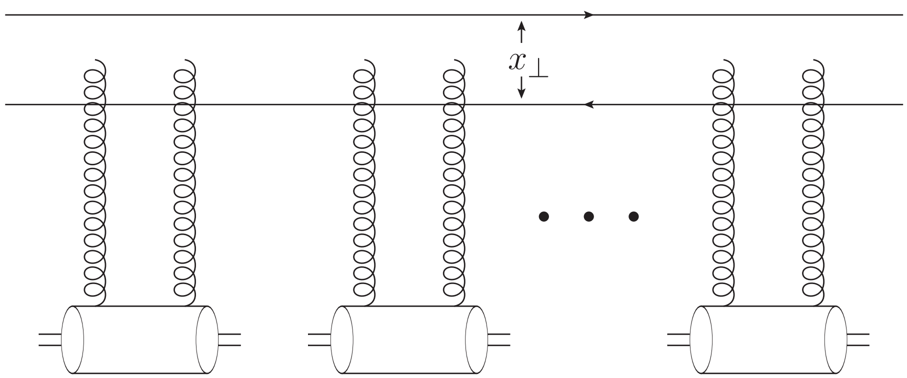

A.H. Mueller, ‘90

Lowest-order interaction with each nucleon – two gluon exchange – lead to the following resummation parameter:

$$\alpha_s^2\, A^{1/3}$$

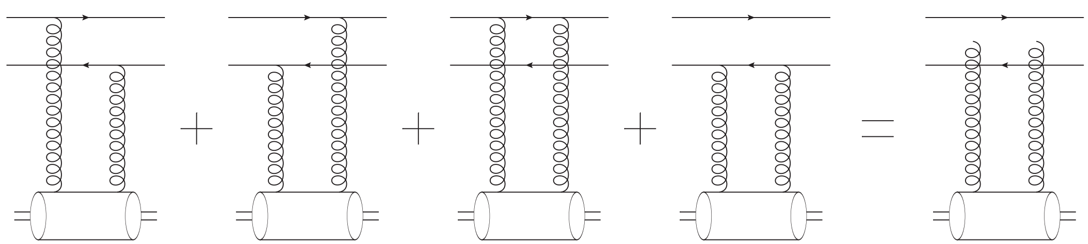

Quasi-classical dipole amplitude

- To resum multiple rescatterings, note that the nucleons are independent of each other and rescatterings on the nucleons are also independent.
- One then writes an equation (Mueller '90)

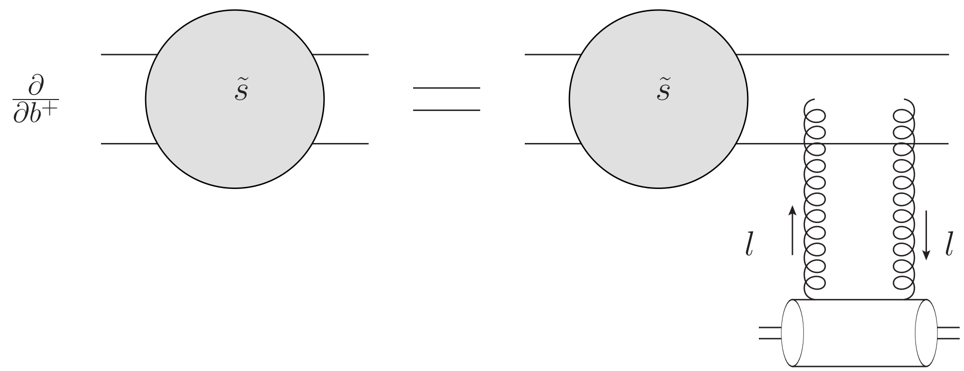

Each scattering!

$$N(x_\perp, Y) = 1 - \exp\left[-\frac{x_\perp^2\, Q_s^2}{4}\, \ln\frac{1}{x_\perp\, \Lambda}\right]$$

DIS in the Classical Approximation

$$\sigma^{q\bar{q}A} = 2 \int d^2b \, N(x_\perp, b_\perp, Y)$$

The dipole-nucleus amplitude in the classical approximation is

$$N(x_\perp, Y) = 1 - \exp\left[-\frac{x_\perp^2 Q_s^2}{4} \ln \frac{1}{x_\perp \Lambda}\right]$$

A.H. Mueller, ‘90

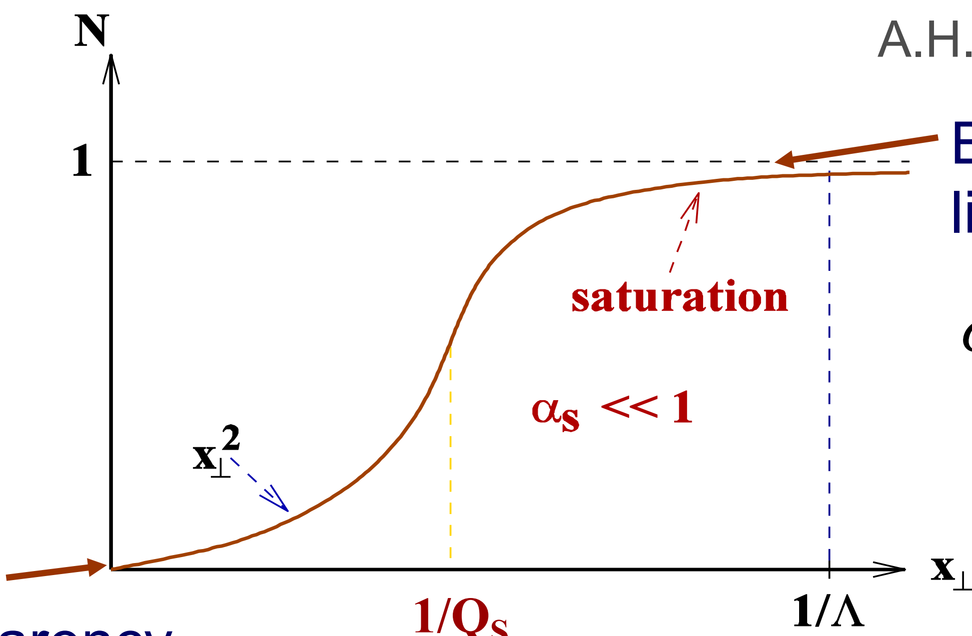

Black disk limit,

$$\sigma_{tot} < 2\pi R^2$$

Color transparency

$Q_s^2 \sim A^{1/3}$

Black Disk Limit

- Start with basic scattering theory: the final and initial states are related by the S-matrix operator,

$$|\psi_f\rangle = \hat{S}\,|\psi_i\rangle$$

- Write it as $$|\psi_f\rangle = |\psi_i\rangle + \left[\hat{S} - 1\right]\,|\psi_i\rangle$$

- The total cross section is

$$\sigma_{tot} \propto \left|\left[\hat{S} - 1\right]\,|\psi_i\rangle\right|^2 = 2 - S - S^*$$

where the forward matrix element of the S-matrix operator is

$$S = \langle\psi_i|\,\hat{S}\,|\psi_i\rangle$$

and we have used unitarity of the S-matrix

$$\hat{S}\,\hat{S}^\dagger = 1$$

Black Disk Limit

- Now, since $$|\psi_f\rangle = |\psi_i\rangle + \left[\hat{S} - 1\right] |\psi_i\rangle$$

  the elastic cross section is

$$\sigma_{el} \propto \left|\langle\psi_i| \left[\hat{S} - 1\right] |\psi_i\rangle\right|^2 = |1 - S|^2$$

- The inelastic cross section can be found via

$$\sigma_{tot} = \sigma_{inel} + \sigma_{el}$$

- In the end, for scattering with impact parameter b we write

$$\sigma_{tot} = 2 \int d^2b \, [1 - \mathrm{Re}\, S(b)]$$

$$\sigma_{el} = \int d^2b \, |1 - S(b)|^2$$

$$\sigma_{inel} = \int d^2b \left[1 - |S(b)|^2\right]$$

Unitarity Limit

- Unitarity implies that

$$1 = \langle\psi_i|\, \hat{S}\, \hat{S}^\dagger\, |\psi_i\rangle = \sum_X \langle\psi_i|\, \hat{S}|X\rangle\, \langle X|\hat{S}^\dagger\, |\psi_i\rangle \geq |S|^2$$

- Therefore

$$|S| \leq 1$$

leading to the unitarity bound on the total cross section

$$\sigma_{tot} = 2\int d^2b\ [1 - \mathrm{Re}\, S(b)] \leq 4\int d^2b = 4\pi R^2$$

- Notice that when S=-1 the inelastic cross section is zero and

$$\sigma_{tot} = 2\int d^2b\,[1 - \mathrm{Re}\, S(b)]$$

$$\sigma_{el} = \int d^2b\,|1 - S(b)|^2$$

$$\sigma_{inel} = \int d^2b\,\left[1 - |S(b)|^2\right]$$

$$\sigma_{tot} = 4\pi R^2 = \sigma_{el}$$

This limit is realized in low-energy scattering!

Black Disk Limit

- At high energy inelastic processes dominate over elastic. Imposing

$$\sigma_{inel} \geq \sigma_{el}$$

we get

$$\mathrm{Re}\, S \geq 0$$

- The bound on the total cross section is (aka the **black disk limit**)

$$\sigma_{tot} = 2 \int d^2b \,[1 - \mathrm{Re}\, S] \leq 2 \int d^2b = 2\pi R^2$$

- The inelastic and elastic cross sections at the black disk limit are

$$\sigma_{inel} = \sigma_{el} = \pi R^2$$

$$\sigma_{tot} = 2 \int d^2b \,[1 - \mathrm{Re}\, S(b)]$$

$$\sigma_{el} = \int d^2b \,|1 - S(b)|^2$$

$$\sigma_{inel} = \int d^2b \left[1 - |S(b)|^2\right]$$

Notation

- At high energies $$\mathrm{Im}\, S \approx 0$$

  Define the dipole amplitude N as the imaginary part of the dipole T-matrix (S=1+iT), such that
  $$\mathrm{Re}\, S = 1 - N$$

- The cross sections are
$$\sigma_{tot} = 2 \int d^2 b\, N(x_\perp, b_\perp)$$
$$\sigma_{el} = \int d^2 b\, N^2(x_\perp, b_\perp)$$
$$\sigma_{inel} = \int d^2 b \left[2\, N(x_\perp, b_\perp) - N^2(x_\perp, b_\perp)\right]$$

- We see that N=1 is the black disk limit. Hence $N \leq 1$ as we saw above.

DIS in the Classical Approximation

The dipole-nucleus amplitude in the classical approximation is

$$N(x_\perp, Y) = 1 - \exp\left[-\frac{x_\perp^2 Q_s^2}{4} \ln\frac{1}{x_\perp \Lambda}\right]$$

A.H. Mueller, '90

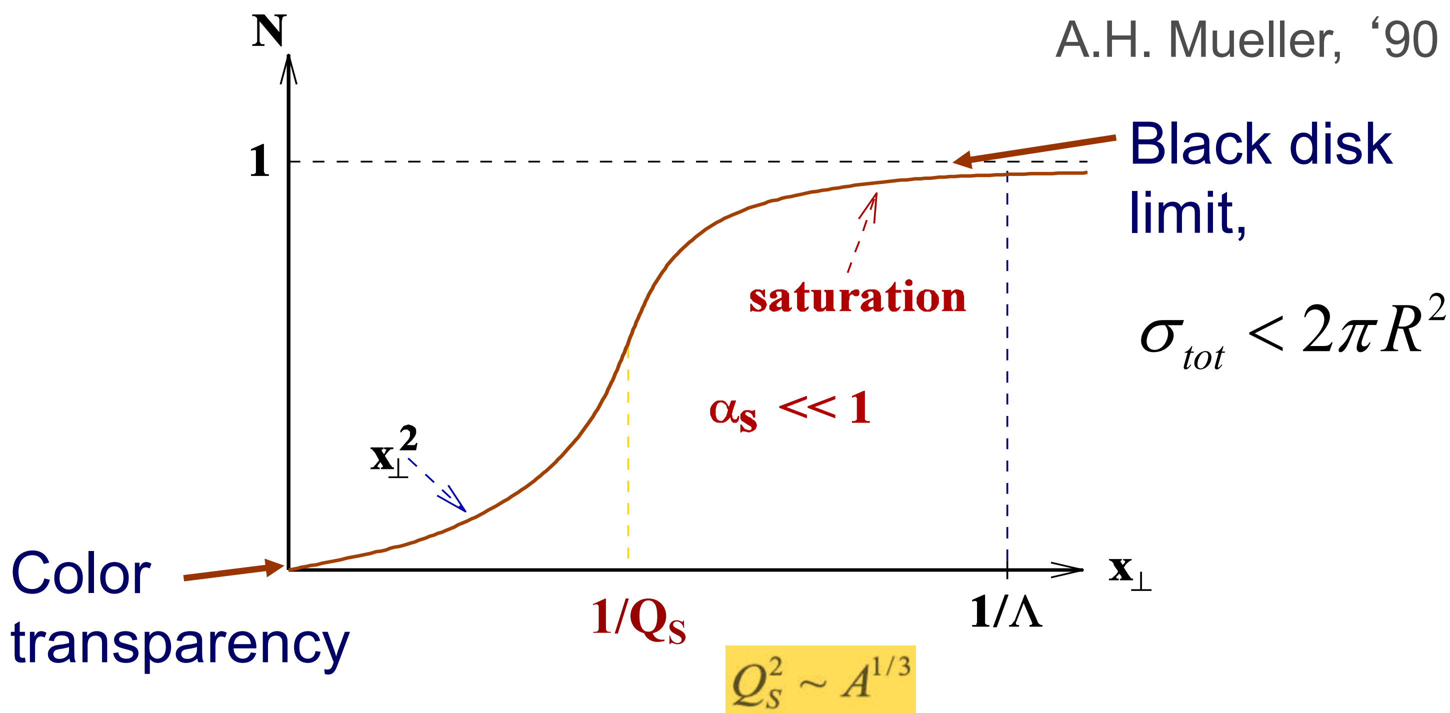

B. McLerran-Venugopalan Model

Gluons at Small-x

- There is a large number of small-x gluons (and quarks) in a proton:

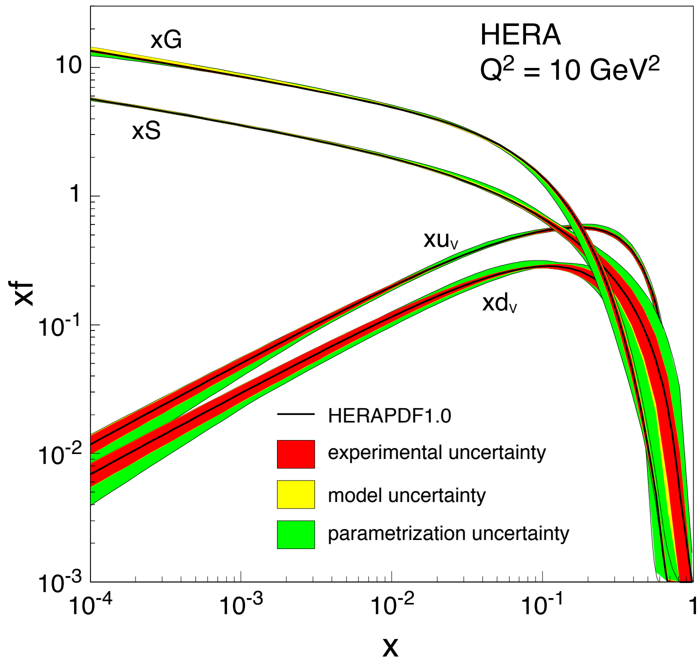

- $G(x, Q^2)$, $q(x, Q^2)$ = gluon and quark number densities (q=u,d, or S for sea).

McLerran-Venugopalan Model

- The wave function of a single nucleus has many small-x quarks and gluons in it.
- In the transverse plane the nucleus is densely packed with gluons and quarks.

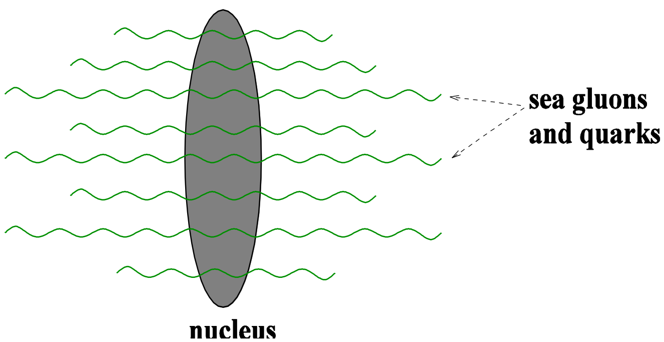

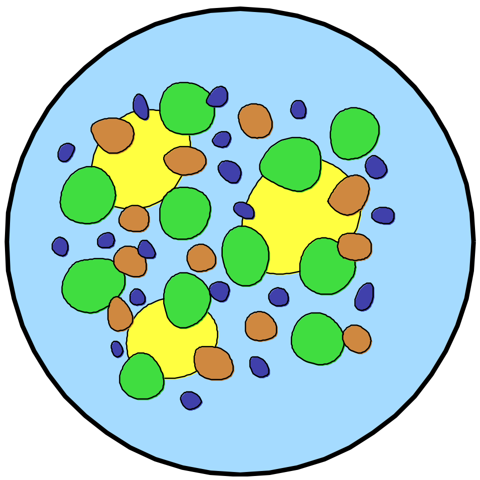

Large occupation number ⇨ Classical Field

McLerran-Venugopalan Model

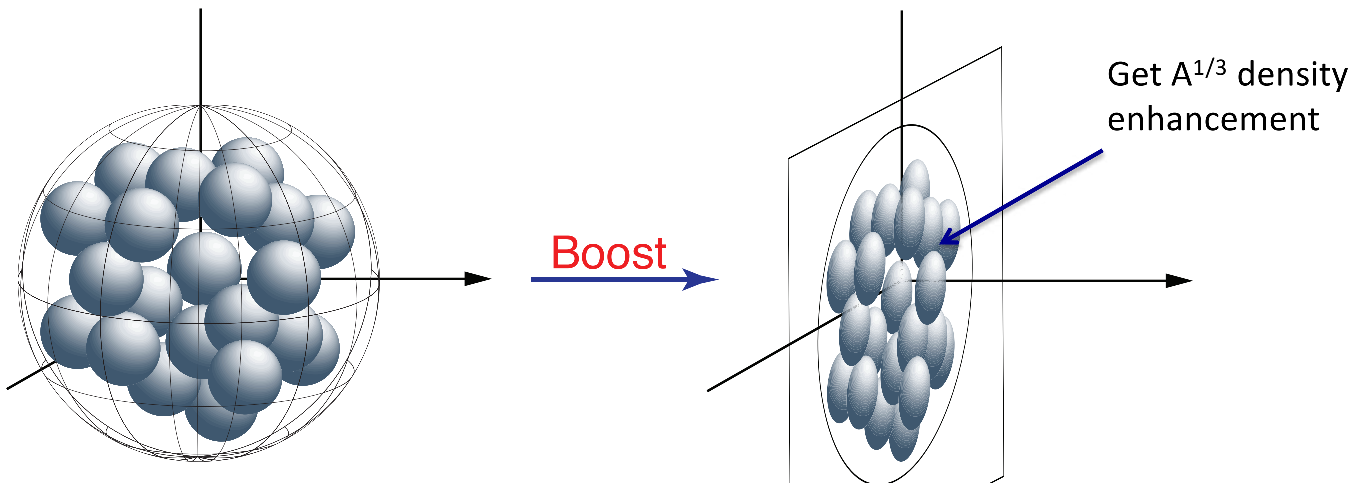

$$M = \rho V = \rho \frac{4}{3}\pi R^3 \sim A \quad \Rightarrow \quad R \sim A^{1/3}$$

$$Q_S^2 \sim A^{1/3}$$

- Large gluon density gives a large momentum scale Q_s (the saturation scale): Q_s^2 ~ # gluons per unit transverse area ~ $A^{1/3}$ (nuclear oomph).
- For $Q_s \gg \Lambda_{QCD}$, get a theory at weak coupling $\alpha_s(Q_s^2) \ll 1$ and the leading gluon field is classical.

Color Charge Density

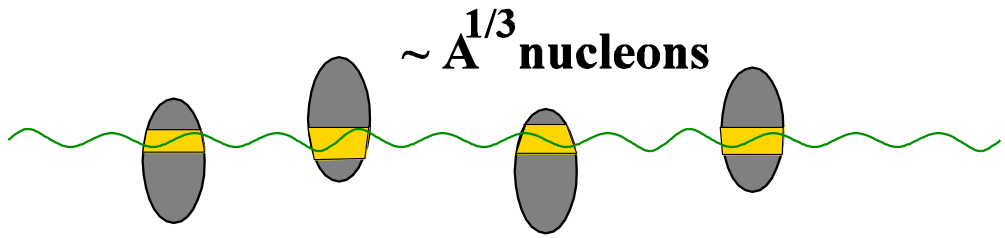

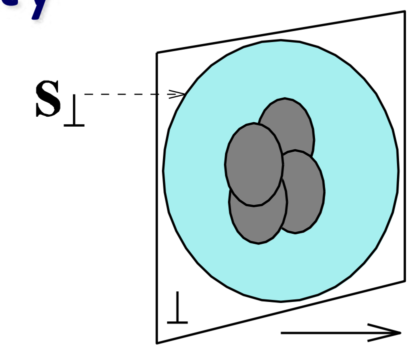

Small-x gluon "sees" the whole nucleus coherently in the longitudinal direction! It "sees" many color charges which form a net effective color charge Q = g (# charges)$^{1/2}$, such that $Q^2 = g^2$ #charges (random walk).

Define color charge density

$$\mu^2 = \frac{Q^2}{S_\perp} = \frac{g^2 \ \# \, charges}{S_\perp} \propto g^2 \, \frac{A}{S_\perp} \propto A^{1/3}$$

McLerran
Venugopalan
`93-`94

such that for a large nucleus (A>>1)

$$\mu^2 \propto \Lambda_{QCD}^2 \, A^{1/3} \gg \Lambda_{QCD}^2 \quad \Longrightarrow \quad \alpha_s(\mu^2) \ll 1$$

Nuclear small-x wave function is perturbative!

$$\mu = Q_s$$

Saturation Scale

To argue that $Q_s^2 \sim A^{1/3}$ let us consider an example of a particle scattering on a nucleus. As it travels through the nucleus it bumps into nucleons. Along a straight line trajectory it encounters $\sim R \sim A^{1/3}$ nucleons, with R the nuclear radius and A the atomic number of the nucleus.

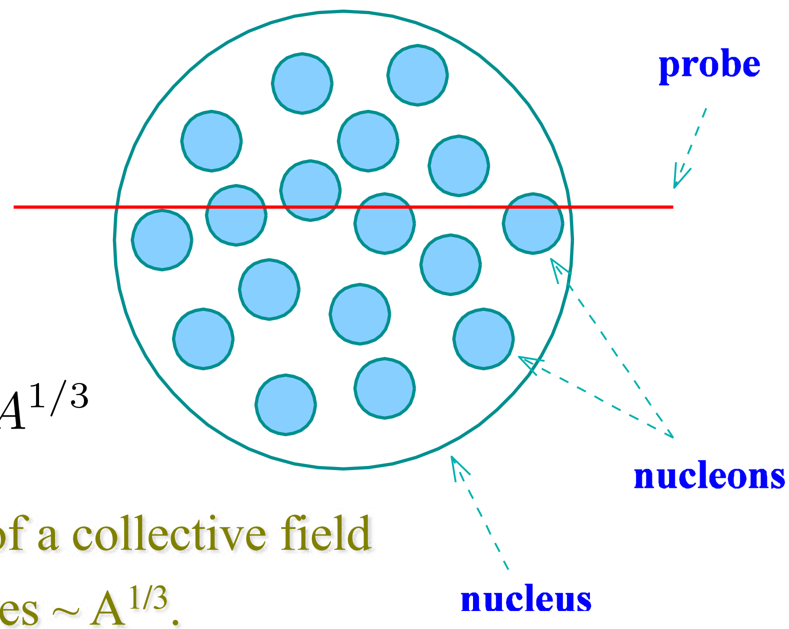

The particle receives $\sim A^{1/3}$ random kicks. Its momentum gets broadened by

$$\Delta k \sim \sqrt{A^{1/3}} \Rightarrow (\Delta k)^2 \sim A^{1/3}$$

Saturation scale, as a feature of a collective field of the whole nucleus also scales $\sim A^{1/3}$.

McLerran-Venugopalan Model

- To find the classical gluon field A_μ of the nucleus one has to solve the non-linear analogue of Maxwell equations – the Yang-Mills equations, with the nucleus as a source of the color charge:

$$\mathcal{D}_\nu \, F^{\mu\nu} = J^\mu$$

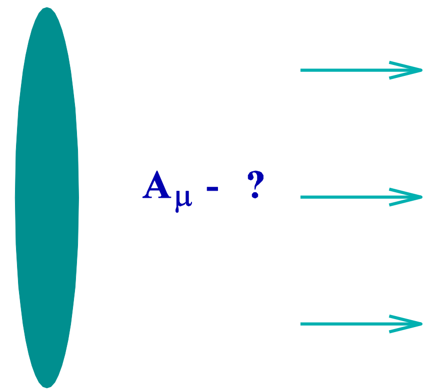

nucleus is Lorentz contacted into a pancake

Yu. K. ’96; J. Jalilian-Marian et al, ‘96

Classical Field of a Nucleus

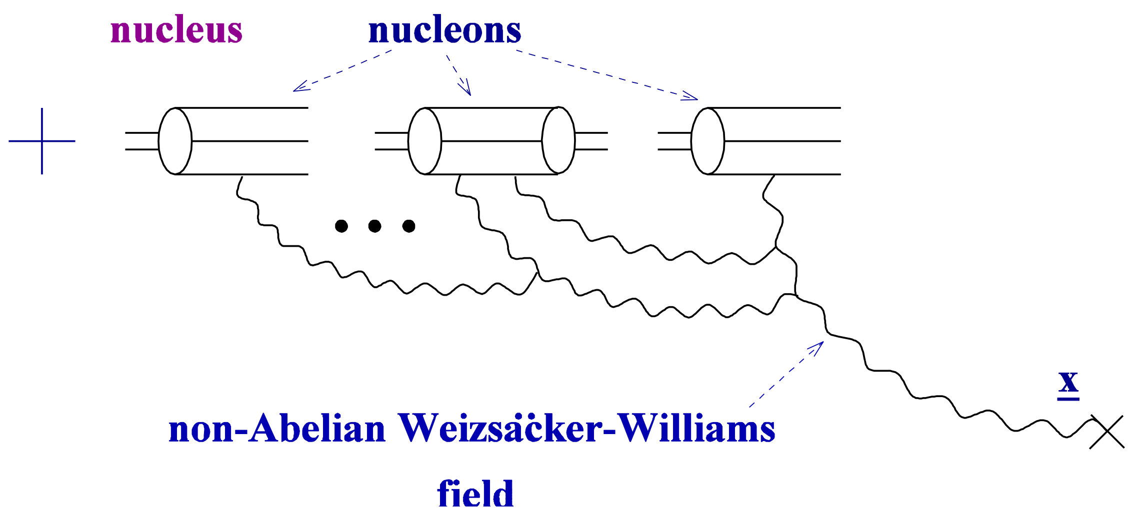

Here's one of the diagrams showing the non-Abelian gluon field of a large nucleus.

The resummation parameter is $\alpha_S^2 A^{1/3}$, corresponding to two gluons per nucleon approximation.

Unpolarized WW Gluon TMD

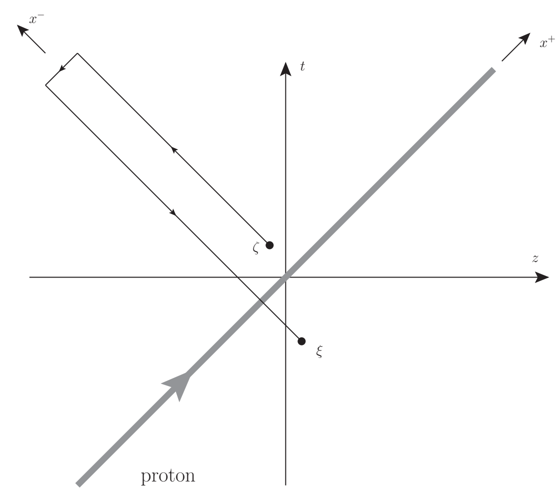

- One can calculate the unpolarized gluon TMD with, say, the forward-pointing (SIDIS) Wilson line staple

$$f^G(x, k_T^2) = \frac{2}{xP^+(2\pi)^3} \int dx^- d^2 x_\perp \, e^{ixP^+ x^- - i\vec{k}_T \cdot \vec{x}_\perp} \left\langle P \middle| \text{tr} \left[F^{+i}(0) \, \mathcal{U}^{[+]}[0, x] \, F^{+i}(x^-, \vec{x}_\perp) \right] \middle| P \right\rangle$$

- In $A^+=0$ gauge one can choose a sub-gauge eliminating the Wilson line staple (making it 1), and, since $F^{+i} = \partial_- A^i$, one obtains

$$f^G(x, k_T^2) = \frac{2xP^+}{(2\pi)^3} \int dx^- d^2 x_\perp \, e^{ixP^+ x^- - i\vec{k}_T \cdot \vec{x}_\perp} \left\langle P \middle| \text{tr} \left[A^i(0) \, A^i(x^-, \vec{x}_\perp) \right] \middle| P \right\rangle$$

- Since the classical (Weizsacker-Williams) A^i field is known exactly from solving the Yang-Mills equations, one can directly calculate the gluon TMD in the classical limit.
- This is the WW gluon TMD.

Classical Gluon Field of a Nucleus

Using the obtained classical gluon field one can construct corresponding gluon distribution function (gluon WW TMD):

$$\phi_A(x,k^2) \sim \left\langle \underline{A}(-k) \cdot \underline{A}(k) \right\rangle$$

with the field in the $A^+=0$ gauge

$$\phi(x,k_T^2) = x\,\pi\, f^G(x,k_T^2)$$

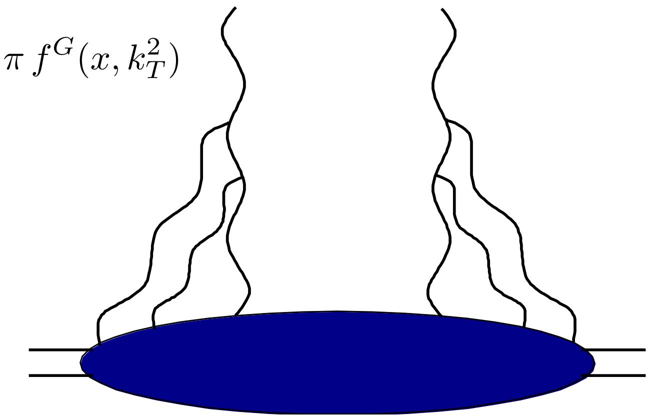

$$\phi_A(x,k_T^2) = \frac{C_F}{\alpha_s\,\pi} \int \frac{d^2x_\perp}{x_\perp^2}\, e^{i\,\underline{k}\cdot\underline{x}} \left[1 - \exp\left(-\frac{x_\perp^2\,Q_s^2}{4}\,\ln\frac{1}{x_\perp\,\Lambda}\right)\right]$$

J. Jalilian-Marian et al, '97; Yu. K. and A. Mueller, '98

⇨ $Q_S=\mu$ is the saturation scale $Q_S^2 \sim A^{1/3}$

⇨ Note that $\phi\sim\langle A_\mu A_\mu\rangle\sim 1/\alpha$ such that $A_\mu\sim 1/g$, which is what one would expect for a classical field.

$$\phi_A(x,k_T^2) = \frac{C_F}{\alpha_s\,\pi}\int \frac{d^2x_\perp}{x_\perp^2}\, e^{i\,\underline{k}\cdot\underline{x}}\left[1-\exp\left(-\frac{x_\perp^2\,Q_s^2}{4}\,\ln\frac{1}{x_\perp\,\Lambda}\right)\right]$$

⇨ In the UV limit of k→∞,

x_T is small and one obtains

$$\phi_A(x,k_T^2) \sim \int d^2x_\perp\, e^{i\,\underline{k}\cdot\underline{x}}\, Q_s^2\,\ln\frac{1}{x_\perp\,\Lambda} \propto \frac{Q_s^2}{k_T^2}$$

which is the usual LO result.

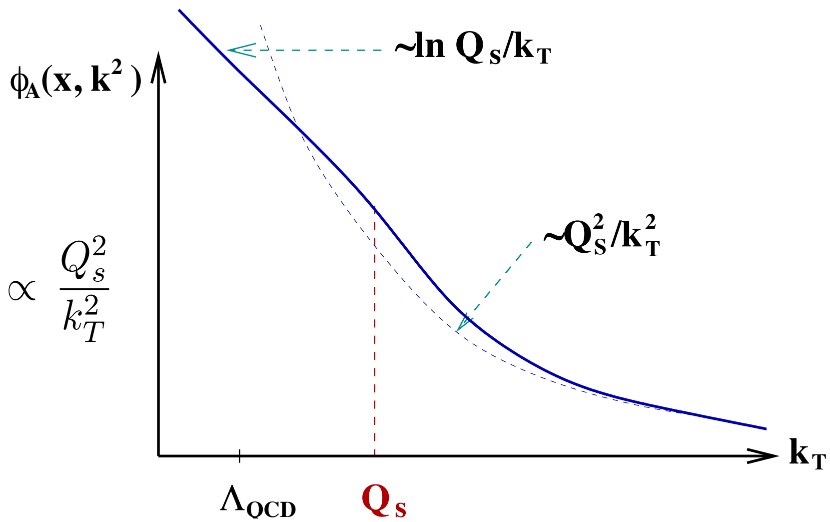

⇨ In the IR limit of small k_T,

x_T is large and we get

$$\phi_A(x,k_T^2) \approx \frac{C_F}{\alpha_s\,\pi}\int_{1/Q_s} \frac{d^2x_\perp}{x_\perp^2}\, e^{i\,\underline{k}\cdot\underline{x}} \propto \ln\frac{Q_s}{k_T}$$

SATURATION !

Divergence is regularized.

Classical Gluon Distribution

A good object to plot is the classical gluon TMD distribution multiplied by the phase space k_T:

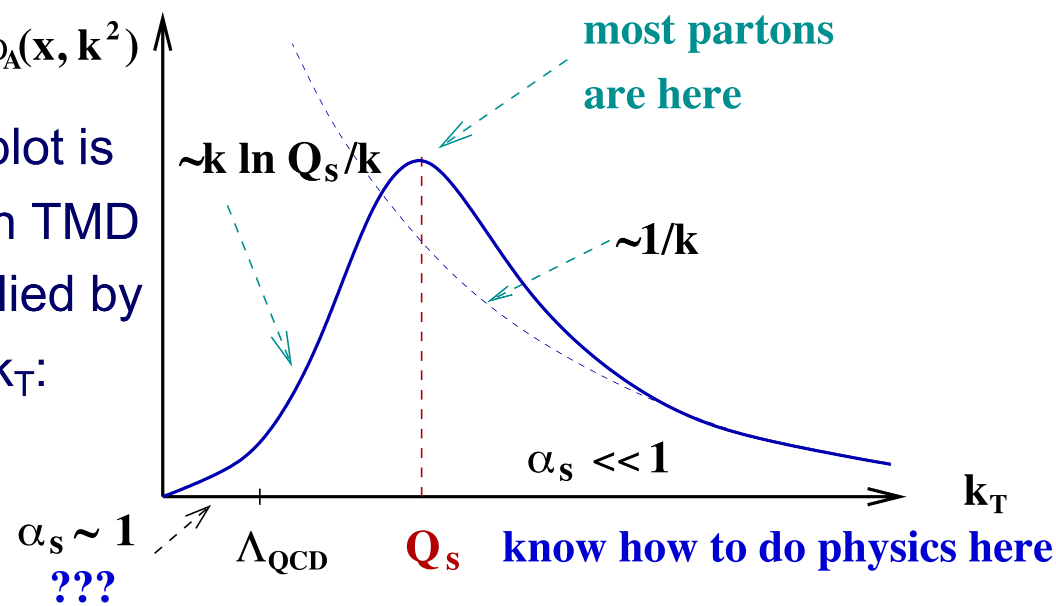

⇨ Most gluons in the nuclear wave function have transverse momentum of the order of $k_T \sim Q_S$ and $Q_S^2 \sim A^{1/3}$

⇨ We have a small coupling description of the whole wave function in the classical approximation.

Summary

- We applied the quasi-classical small-*x* approach to DIS in the dipole picture, obtaining Glauber-Mueller formula for multiple rescatterings of a dipole in a nucleus.

- We saw that onset of saturation ensures that unitarity (the black disk limit) is not violated. Saturation is a consequence of unitarity!

- We have reviewed the McLerran-Venugopalan model for the small-*x* wave function of a large nucleus.

- We saw the onset of gluon saturation and the appearance of a large transverse momentum scale – the saturation scale:

$$Q_s^2 \sim A^{1/3}$$

Summary of the last time

- We discussed dipole picture of DIS:

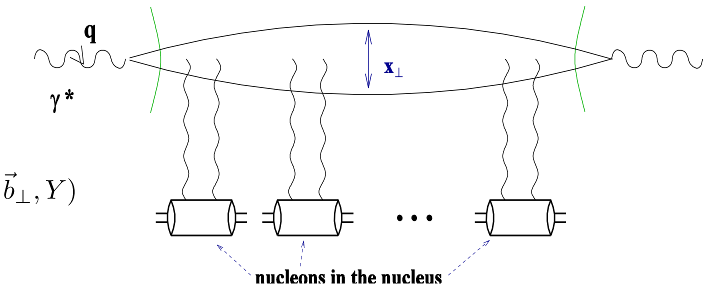

$$\sigma_{tot}^{\gamma^* A} = \int \frac{d^2 x_\perp}{2\,\pi}\, d^2 b_\perp \int\limits_0^1 \frac{dz}{z\,(1-z)}\; |\Psi^{\gamma^* \to q\bar{q}}(\vec{x}_\perp, z)|^2 \; N(\vec{x}_\perp, \vec{b}_\perp, Y)$$

- We calculated multiple-rescattering of the dipole on a nucleus: $Q_S^2 \sim A^{1/3}$

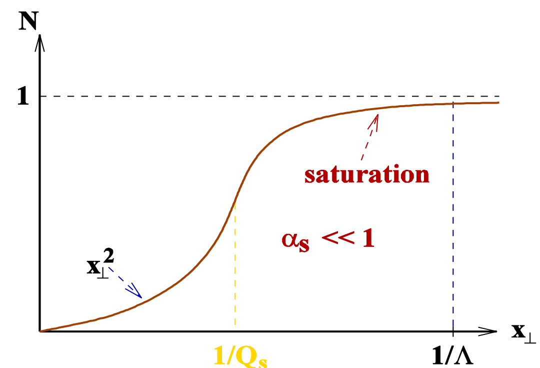

- We discussed the MV model, in which the gluon field of the proton/nucleus is classical, such that you can calculate the WW gluon TMD directly:

$$\phi_A(x, k_T^2) = \frac{C_F}{\alpha_s\,\pi} \int \frac{d^2 x_\perp}{x_\perp^2}\, e^{i\,\underline{k}\cdot\underline{x}} \left[1 - \exp\left(- \frac{x_\perp^2\, Q_s^2}{4} \ln \frac{1}{x_\perp\,\Lambda} \right) \right]$$

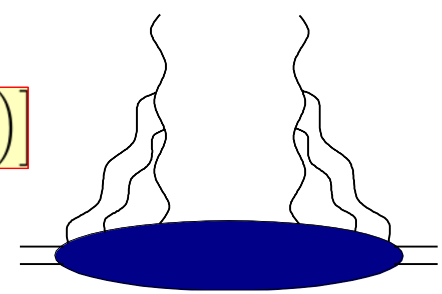

Small-x evolution equations

Small-x Evolution

- Energy dependence comes in through the long-lived *s*-channel gluon corrections (higher Fock states):

$$\alpha_s \ \ln s \sim \alpha_s \ \ln \frac{1}{x} \sim 1$$

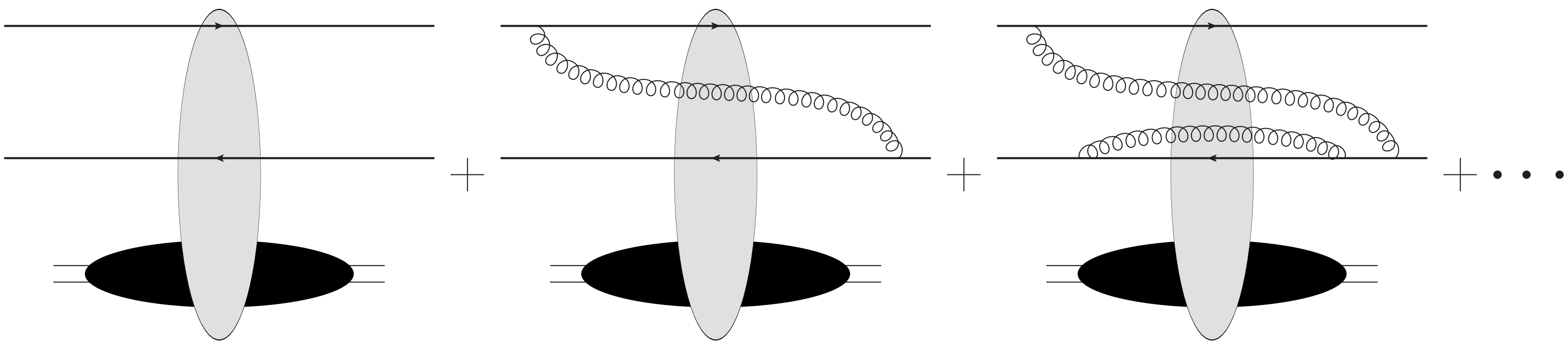

These extra gluons bring in powers of α_S ln s, such that when α_S << 1 and ln s >>1 this parameter is α_S ln s ~ 1 (leading logarithmic approximation, LLA).

Small-x Evolution: Large N_c Limit

- How do we resum this cascade of gluons?
- The simplification comes from the large-Nc limit, where each gluon becomes a quark-antiquark pair:

$$3 \otimes \bar{3} = 1 \oplus 8 \quad \Rightarrow \quad N_c \otimes \bar{N}_c = 1 \oplus (N_c^2 - 1) \approx N_c^2 - 1$$

- Gluon cascade becomes a dipole cascade (each color outlines a dipole):

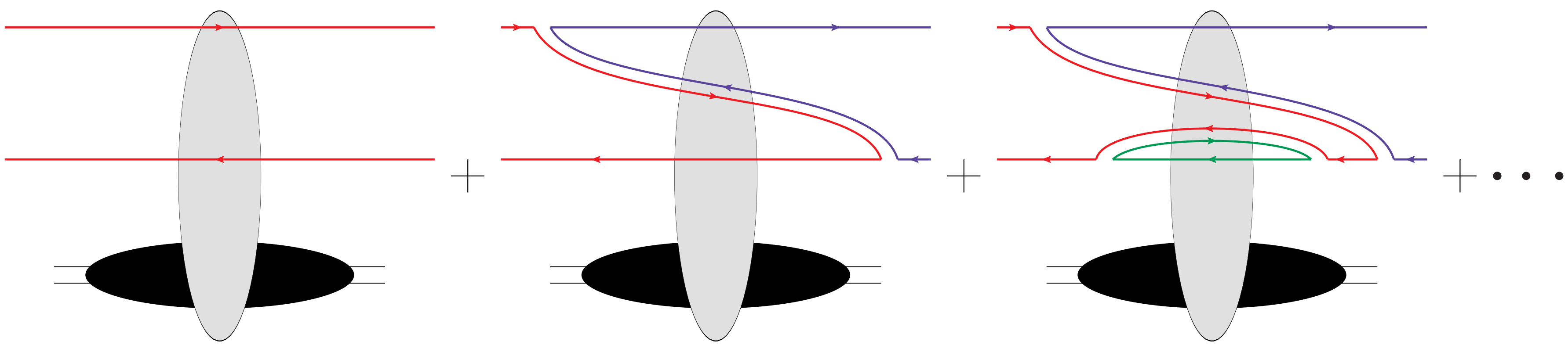

Mueller's Dipole Model

To include the quantum evolution in a dipole amplitude one
Can use the approach developed by A. H. Mueller in '93-'94.
The goal is to resum leading logs of energy, α log s, just like
for the BFKL equation.

Emission of a small-x gluon taken in the large-N_C limit would split the original color dipole in two:

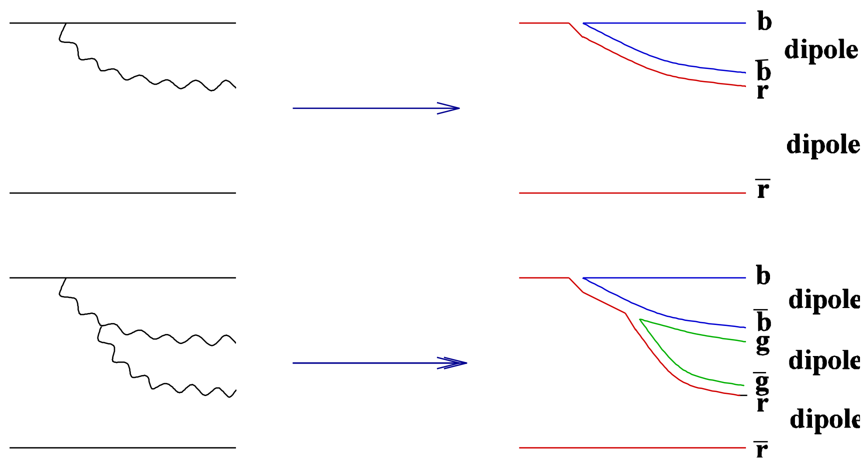

$$3 \otimes \bar{3} = 1 \oplus 8 \quad \Rightarrow \quad N_c \otimes \bar{N}_c = 1 \oplus (N_c^2 - 1) \approx N_c^2 - 1$$

Notation (Large-N_c)

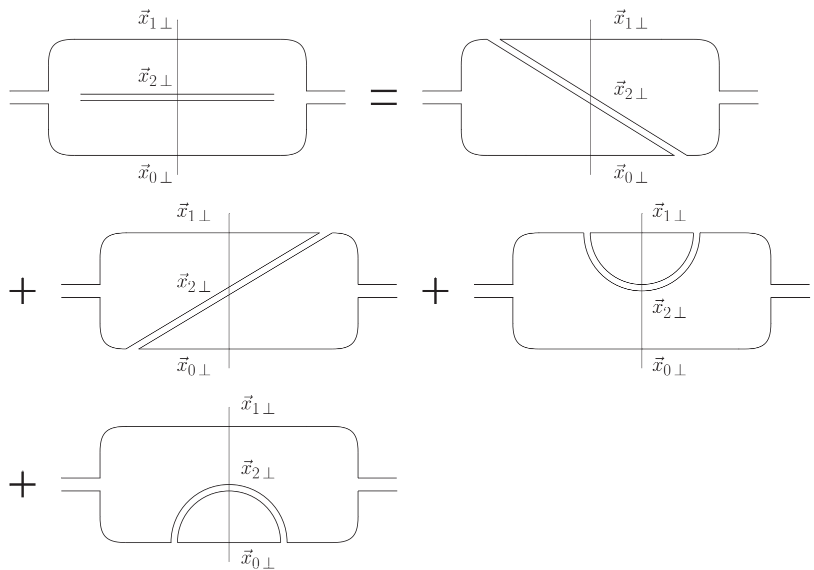

Real emissions in the amplitude squared

(dashed line – all Glauber-Mueller exchanges at light-cone time =0)

Virtual corrections in the amplitude (wave function)

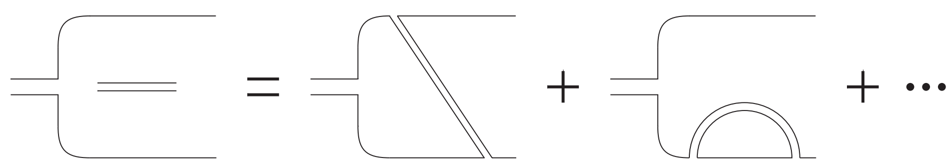

Nonlinear Evolution

To sum up the gluon cascade at large-N_C we write the following equation for the dipole S-matrix:

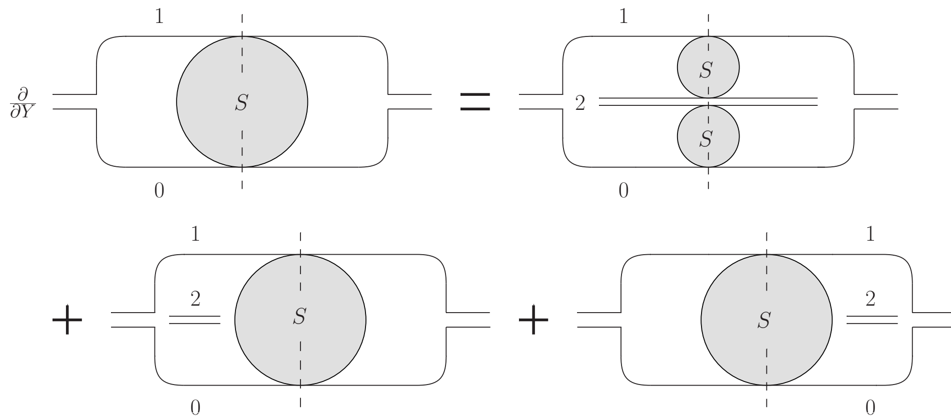

dashed line = all interactions with the target

$$Y = \ln \frac{1}{x} \sim \ln s$$

$$\partial_Y S_{\mathbf{x}_0,\mathbf{x}_1}(Y) = \frac{\alpha_s N_c}{2\pi^2} \int d^2 x_2 \frac{x_{01}^2}{x_{02}^2 \, x_{21}^2} \left[S_{\mathbf{x}_0,\mathbf{x}_2}(Y) \, S_{\mathbf{x}_2,\mathbf{x}_1}(Y) - S_{\mathbf{x}_0,\mathbf{x}_1}(Y)\right]$$

Remembering that S=1 + i T = 1 - N where N = Im(T) we can rewrite this equation in terms of the dipole scattering amplitude N.

Nonlinear evolution at large N_c

As N=1-S we write

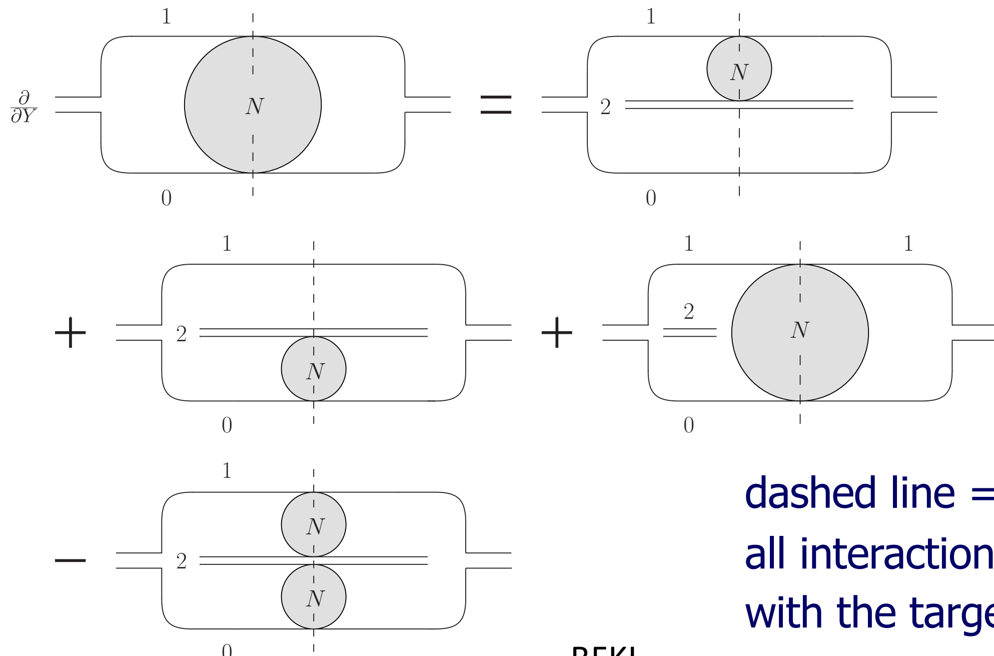

dashed line = all interactions with the target

$$\partial_Y N_{\mathbf{x}_0,\mathbf{x}_1}(Y) = \frac{\alpha_s N_c}{2\pi^2} \int d^2 x_2 \, \frac{x_{01}^2}{x_{02}^2 \, x_{21}^2} \, [\overbrace{N_{\mathbf{x}_0,\mathbf{x}_2}(Y) + N_{\mathbf{x}_2,\mathbf{x}_1}(Y) - N_{\mathbf{x}_0,\mathbf{x}_1}(Y)}^{\text{BFKL}} - N_{\mathbf{x}_0,\mathbf{x}_2}(Y) \, N_{\mathbf{x}_2,\mathbf{x}_1}(Y)]$$

Balitsky ‘96, Yu.K. ’99; beyond large N_c, JIMWLK evolution, 0.1% correction for the dipole amplitude

Re-summing gluon cascade

- At large N_c the gluon cascade turns into a dipole cascade. We are resumming the dipole cascade, with each dipole interacting with the target independently:

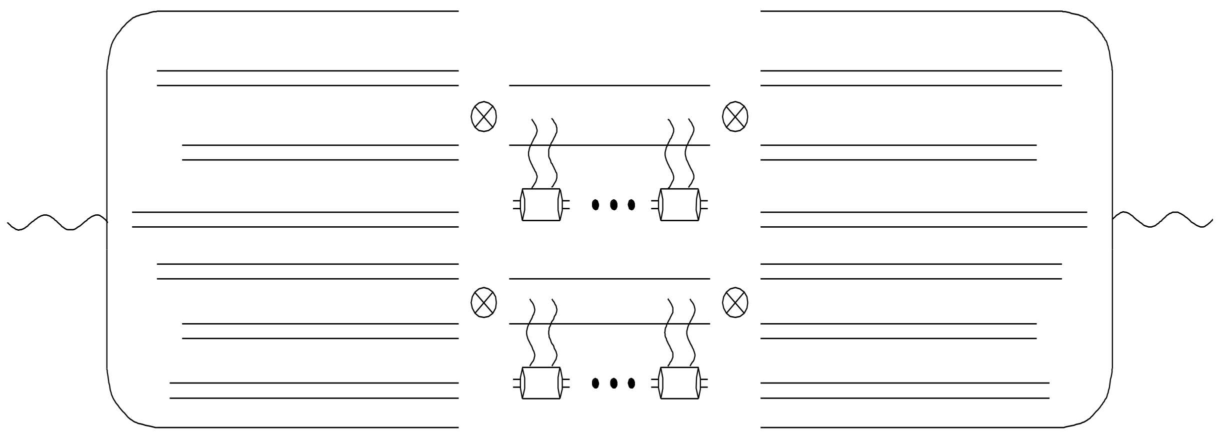

Resummation parameter

- BK equation resums powers of

$$\alpha_s \, N_c \, Y$$

- The Glauber-Mueller/McLerran-Venugopalan initial conditions resum powers of

$$\alpha_s^2 \, A^{1/3}$$

- Beyond the large-N_c limit: use the JIMWLK functional evolution equation (Iancu, Jalilian-Marian, Kovner, Leonidov, McLerran and Weigert, 1997-2002)

JIMWLK: derivation outline

A.H. Mueller, 2001

- Start by introducing a weight functional, $W_Y[\alpha]$. Here $\alpha = A^+$ is the gluon field of the target proton or nucleus. $\alpha(x^-, \vec{x}) \equiv A^+(x^+ = 0, x^-, \vec{x})$
- The functional is used to generate expectation values of gluon-field dependent operators in the target state:

$$\langle \hat{O}_\alpha \rangle_Y = \int \mathcal{D}\alpha \; \hat{O}_\alpha \, W_Y[\alpha]$$

- Imagine that we know small-x evolution for some operator O:

$$\partial_Y \, \langle \hat{O}_\alpha \rangle_Y = \langle \mathcal{K}_\alpha \otimes \hat{O}_\alpha \rangle_Y = \int \mathcal{D}\alpha \, \left[\mathcal{K}_\alpha \otimes \hat{O}_\alpha \right] \, W_Y[\alpha]$$

- On the other hand, we can differentiate the first equation above,

$$\partial_Y \, \langle \hat{O}_\alpha \rangle_Y = \int \mathcal{D}\alpha \; \hat{O}_\alpha \; \partial_Y \, W_Y[\alpha]$$

- Comparing the last two equations and integrating by parts in the second to last equation, we will arrive at and equation for the weight functional $W_Y[\alpha]$.

JIMWLK: derivation outline

- As a test operator, take a pair of Wilson lines (not a dipole!):

$$\hat{O}_{\vec{x}_{1\perp},\vec{x}_{0\perp}} = V_{\vec{x}_{1\perp}} \otimes V^{\dagger}_{\vec{x}_{0\perp}}$$

- Construct the evolution of this operator by summing the following familiar diagrams:

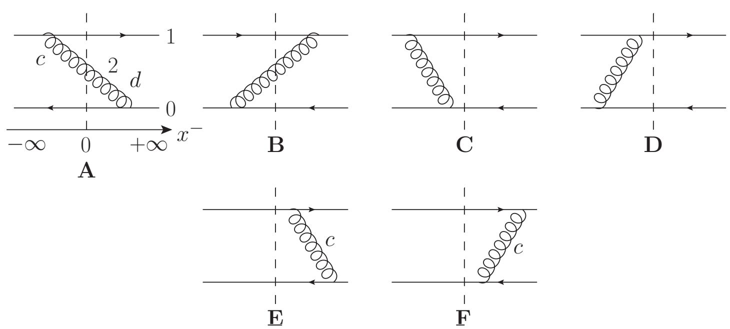

real

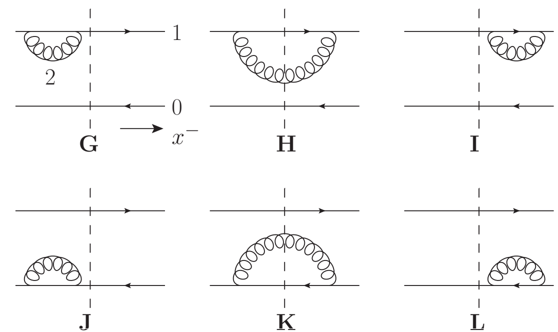

virtual

The JIMWLK Equation

- In the end one arrive at the JIMWLK evolution equation (Jalilian-Marian—Iancu–McLerran—Weigert—Leonidov—Kovner, 1997-2002):

$$\partial_Y W_Y[\alpha] = \alpha_s \left\{ \frac{1}{2} \int d^2 x_\perp \, d^2 y_\perp \, \frac{\delta^2}{\delta \alpha^a(x^-, \vec{x}_\perp) \, \delta \alpha^b(y^-, \vec{y}_\perp)} \left[\eta^{ab}_{\vec{x}_\perp \vec{y}_\perp} W_Y[\alpha] \right] - \int d^2 x_\perp \, \frac{\delta}{\delta \alpha^a(x^-, \vec{x}_\perp)} \left[\nu^a_{\vec{x}_\perp} W_Y[\alpha] \right] \right\}$$

with

$$\eta^{ab}_{\vec{x}_{1\perp} \vec{x}_{0\perp}} = \frac{4}{g^2 \, \pi^2} \int d^2 x_2 \, \frac{\vec{x}_{21} \cdot \vec{x}_{20}}{x_{21}^2 \, x_{20}^2} \left[\mathbf{1} - U_{\vec{x}_{1\perp}} U^\dagger_{\vec{x}_{2\perp}} - U_{\vec{x}_{2\perp}} U^\dagger_{\vec{x}_{0\perp}} + U_{\vec{x}_{1\perp}} U^\dagger_{\vec{x}_{0\perp}} \right]^{ab}$$

$$\nu^a_{\vec{x}_{1\perp}} = \frac{i}{g \, \pi^2} \int \frac{d^2 x_2}{x_{21}^2} \, \mathrm{Tr} \left[T^a U_{\vec{x}_{1\perp}} U^\dagger_{\vec{x}_{2\perp}} \right]$$

- Here U is the adjoint Wilson line on a light cone,

$$U_{\vec{x}_\perp} = \mathrm{P} \exp \left\{ i \, g \int\limits_{-\infty}^{\infty} dx^- \, \mathcal{A}^+(x^+ = 0, x^-, \vec{x}_\perp) \right\}$$

The JIMWLK Equation

- JIMWLK equation can be used to construct any-N_C small-x evolution of any operator made of infinite light-cone Wilson lines (in any representation), such as color-dipole, color-quadrupole, etc., and other operators.

- Since

$$\Box \alpha(x^-, \vec{x}) = \rho(x^-, \vec{x})$$

JIMWLK evolution can be re-written in terms of the color density ρ in the kernel.

- JIMWLK approach sums up powers of $\alpha_s \, Y$ and $\alpha_s^2 \, A^{1/3}$

Solving JIMWLK

- The JIMWLK equation was solved on the lattice by K. Rummukainen and H. Weigert '04 (and others since).
- For the dipole amplitude $N(x_0, x_1, Y)$, the **relative** corrections to the large-N_C limit BK equation are **< 0.001 !** Not the naïve $1/N_C^2 \sim 0.1$! (For realistic rapidities/energies.)
- The reason for that is dynamical and is largely due to saturation effects suppressing the bulk of the potential $1/N_C^2$ corrections (Yu.K., J. Kuokkanen, K. Rummukainen, H. Weigert, '08).
- There are other objects at small x, quadrupoles, double-trace operators, etc. Some (linear combinations) of them are subleading-N_c, and one has to use JIMWLK to describe their evolution.

Solution of the nonlinear equation

Solution of BK equation

We conclude that

$$Q_s^2 \sim \left(\frac{1}{x}\right)^{\lambda}$$

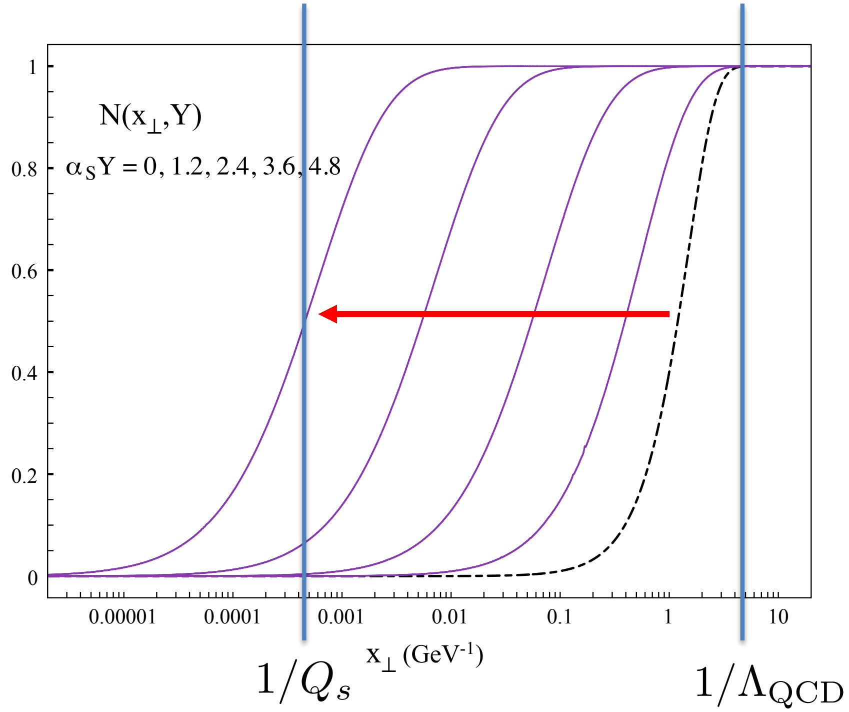

numerical solution
by J. Albacete '03

Energy increases → Q_s increases
moving further away from Λ_{QCD}

BK solution preserves the black disk limit, N<1 always
(unlike the linear BFKL equation)

$$\sigma^{q\bar{q}A} = 2\int d^2b\, N(x_\perp, b_\perp, Y)$$

Saturation scale

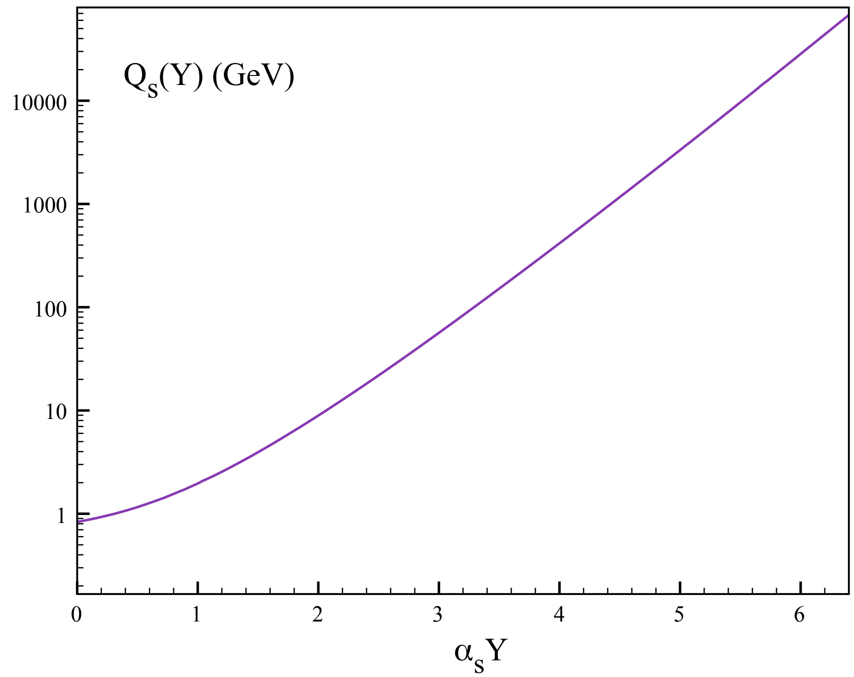

numerical solution by J. Albacete (ca. 2006)

BK Solution

- Preserves the black disk limit, N<1 always.

$$\sigma^{q\bar{q}A} = 2 \int d^2b \, N(x_\perp, b_\perp, Y)$$

- Avoids the IR problem of BFKL evolution due to the saturation scale screening the IR:

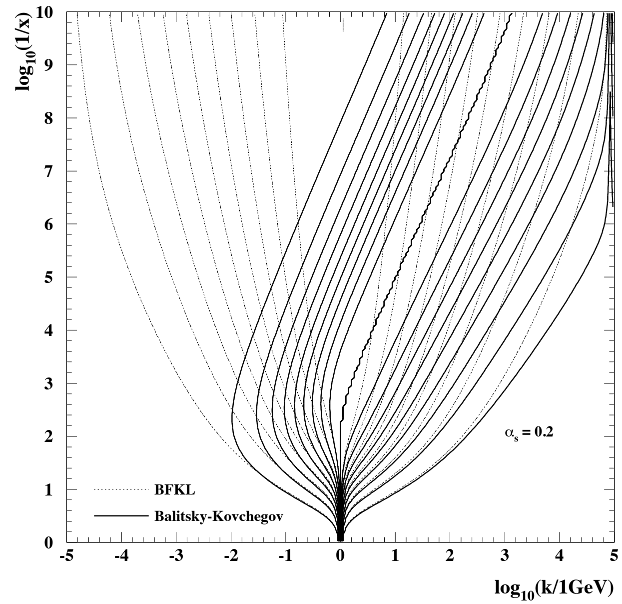

Golec-Biernat, Motyka, Stasto ‘02

The BFKL Equation




- The Balitsky, Fadin, Kuraev, Lipatov (BFKL) equation was derived in 1977-78.
- One starts with a two-gluon exchange diagram (left) and "dresses" it by radiative corrections.
- The leading high-energy contribution can be drawn as a ladder diagram, with the t-channel gluons being the special "reggeized" gluons and the thick dots representing effective Lipatov vertices.

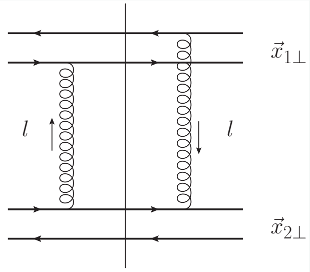

$$\frac{\partial f}{\partial \ln s} = \alpha_s \, K_{BFKL} \otimes f$$

The BFKL equation.
K_{BFKL} is an integral kernel.

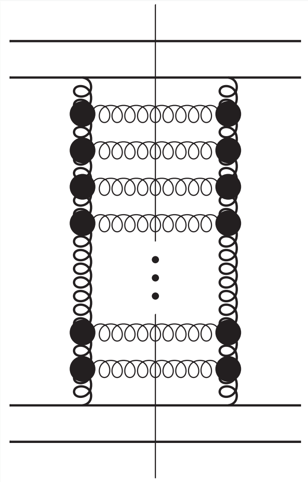

BFKL Equation

In the conventional Feynman-diagram picture the BFKL equation can be represented by the ladder graph shown here. Each rung of the ladder brings in a power of $\alpha \ln s$.

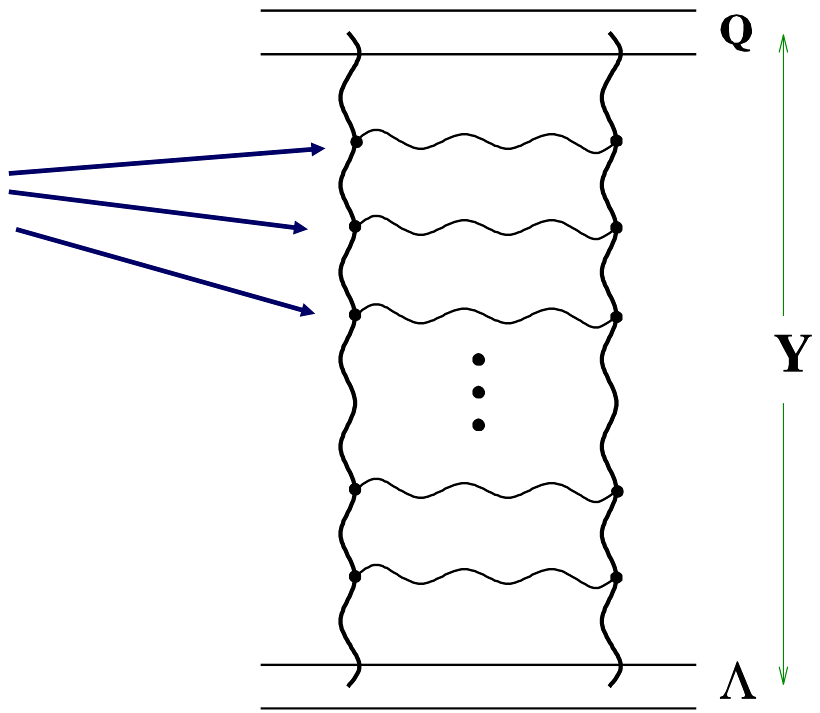

The resulting dipole amplitude grows as a power of energy

$$N \sim s^{\Delta}$$

violating Froissart unitarity bound

$$\sigma_{tot} \leq const \ln^2 s$$

GLR-MQ Equation

Gribov, Levin and Ryskin ('81) proposed summing up "fan" diagrams:

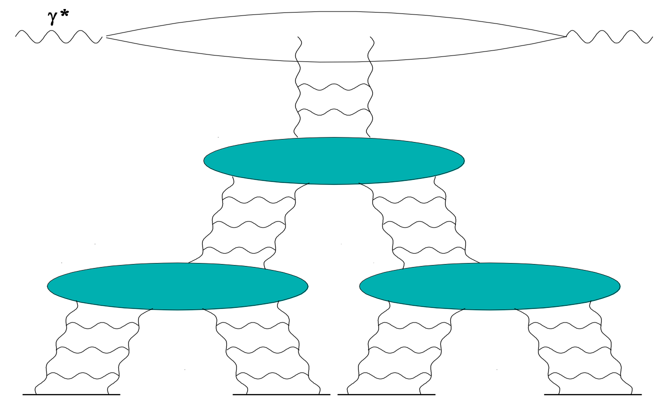

Mueller and Qiu ('85) summed "fan" diagrams for large Q^2.

The GLR-MQ equation reads:

$$\frac{\partial}{\partial \ln 1/x} \phi(x, k_T^2) = \alpha_s K_{BFKL} \otimes \phi(x, k_T^2) - \alpha_s [\phi(x, k_T^2)]^2$$

GLR-MQ equation has the same principle of recombination as BK and JIMWLK. GLR-MQ equation was thought about as the first nonlinear correction to the linear BFKL evolution. An AGL (Ayala, Gay Ducati, Levin '96) equation was suggested to resum higher-order nonlinear corrections.

BK/JIMWLK derivation showed that for the dipole amplitude N (!) there are no more terms in the large-N_C limit and obtained the correct kernel for the non-linear term (compared to GLR suggestion).

Energy Dependence of the Saturation Scale

Single BFKL ladder gives scattering amplitude of the order $N \sim \frac{\Lambda}{k_T} s^{\Delta}$

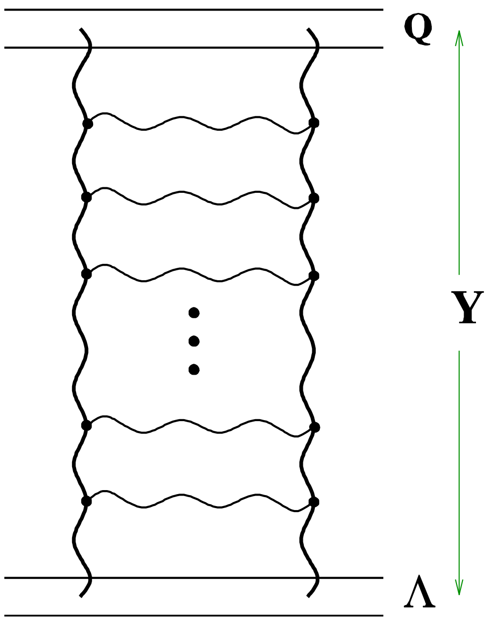

Nonlinear saturation effects become important when N ~ N^2 ⇨ N ~ 1. This happens at $k_T = Q_s \sim \Lambda\, s^{\Delta}$

Saturation scale grows with energy!

Typical partons in the wave function have $k_T \sim Q_S$, so that their characteristic size is of the order $r \sim 1/k_T \sim 1/Q_S$.

⇨ Typical parton size decreases with energy!

Saturation scale

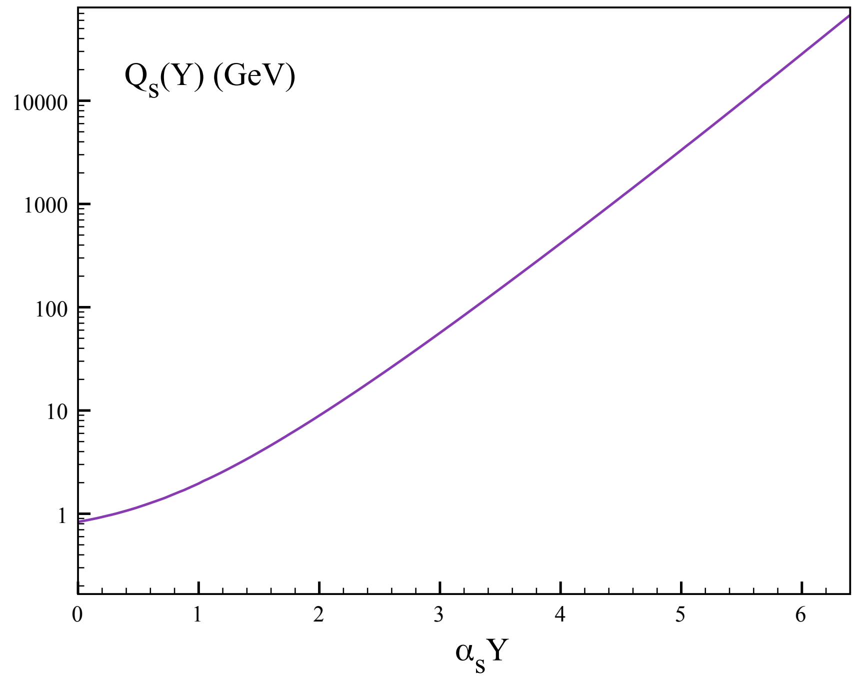

numerical solution by J. Albacete

High Density of Gluons

- High number of gluons populates the transverse extent of the proton or nucleus, leading to a very dense saturated wave function known as the Color Glass Condensate (CGC):

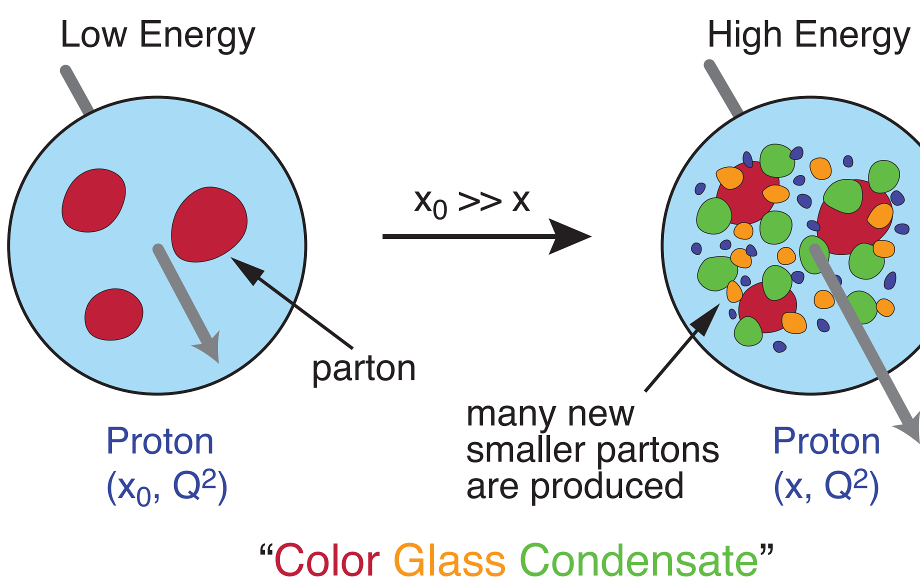

Map of High Energy QCD

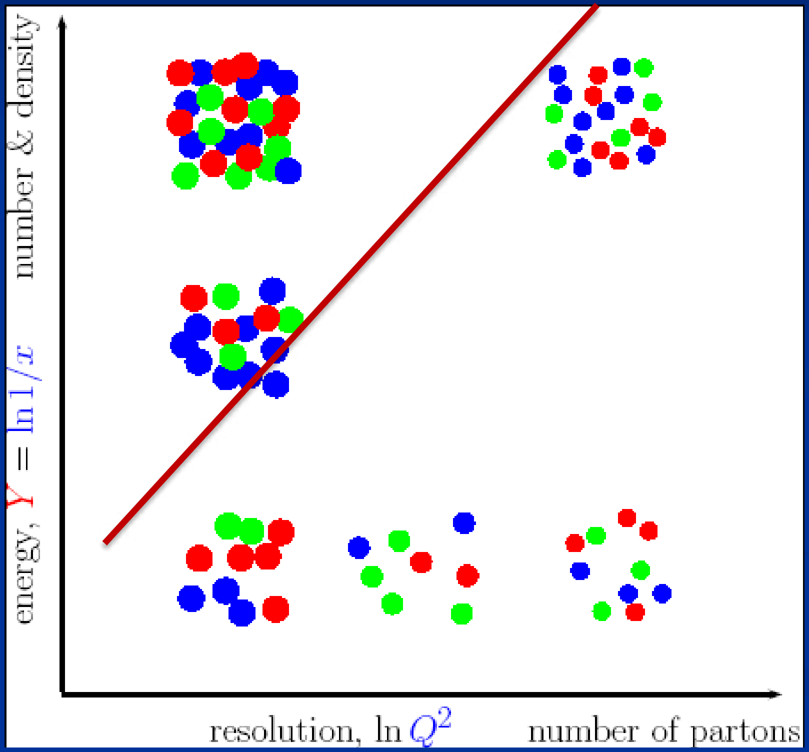

energy

size of gluons

Map of High Energy QCD

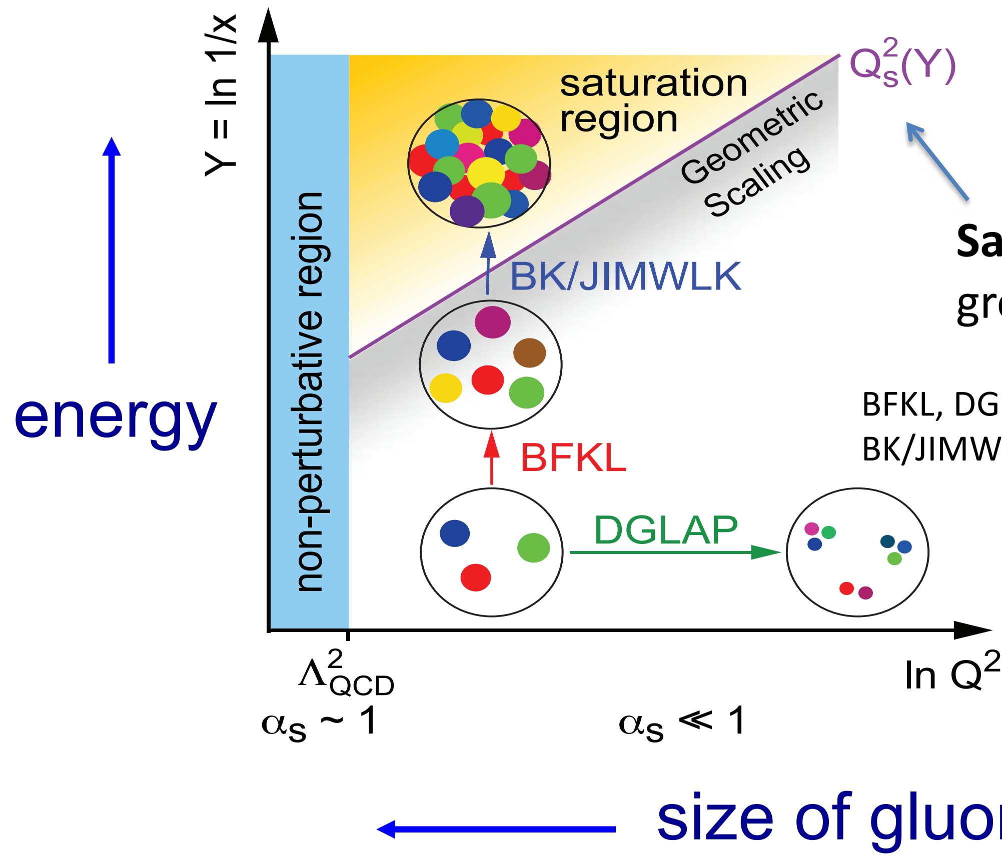

$$Q_s^2 \sim \left(\frac{1}{x}\right)^{\lambda}$$

Saturation Scale
grows with energy

BFKL, DGLAP – linear equations
BK/JIMWLK – nonlinear

Map of High Energy QCD

Saturation Scale
grows with energy and atomic number A for a nucleus

$$Q_s^2 \sim \left(\frac{A}{x}\right)^{1/3}$$

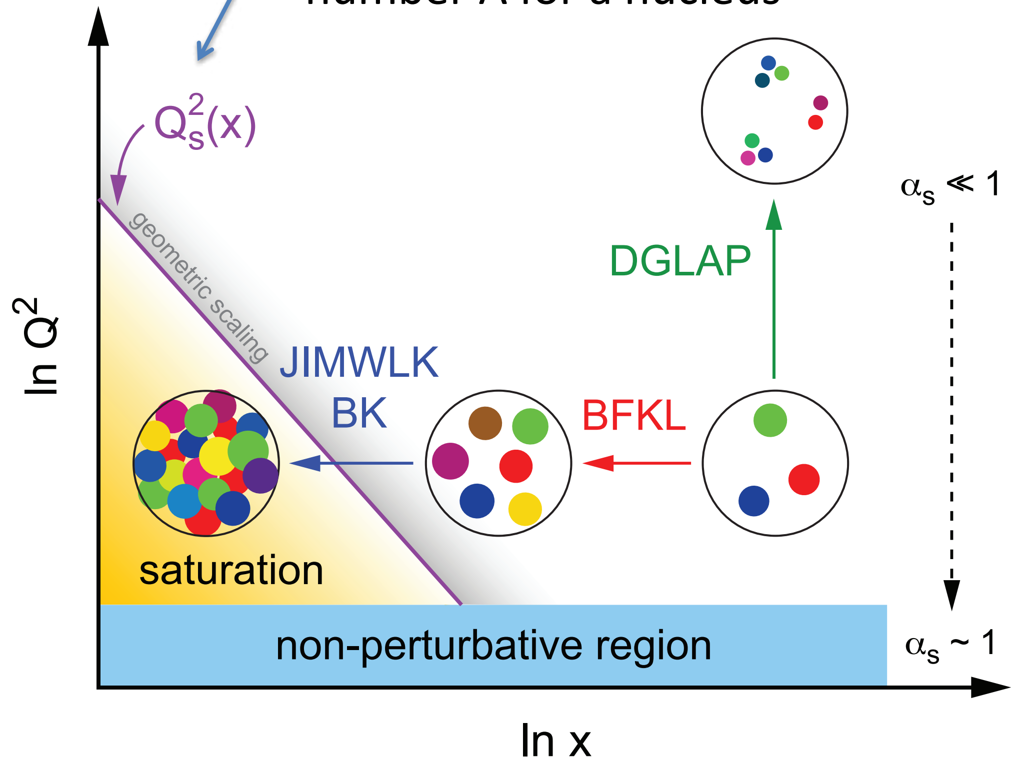

BFKL, DGLAP – linear equations
BK/JIMWLK – nonlinear

Geometric Scaling

- One of the predictions of the JIMWLK/BK evolution equations is geometric scaling:

  DIS cross section should be a function of one parameter:

$$\sigma_{DIS}(x, Q^2) = \sigma_{DIS}(Q^2 / Q_S^2(x))$$

(Levin, Tuchin '99; Iancu, Itakura, McLerran '02)

Geometric Scaling

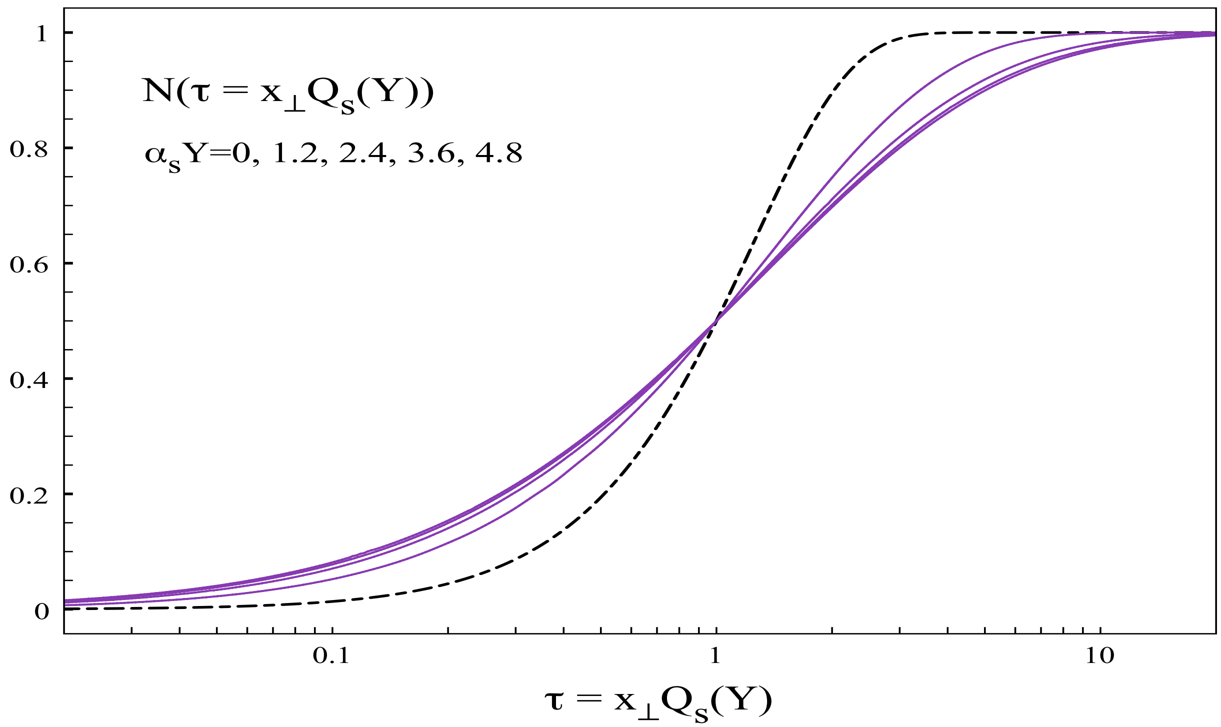

numerical solution by J. Albacete

Geometric Scaling in DIS

Geometric scaling was found in DIS data by Stasto, Golec-Biernat, Kwiecinski in `00.

Here they plot the total DIS cross section, which is a function of 2 variables, Q^2 and x, as a function of just <u>one</u> variable:

$$\tau = \frac{Q^2}{Q_s^2}$$

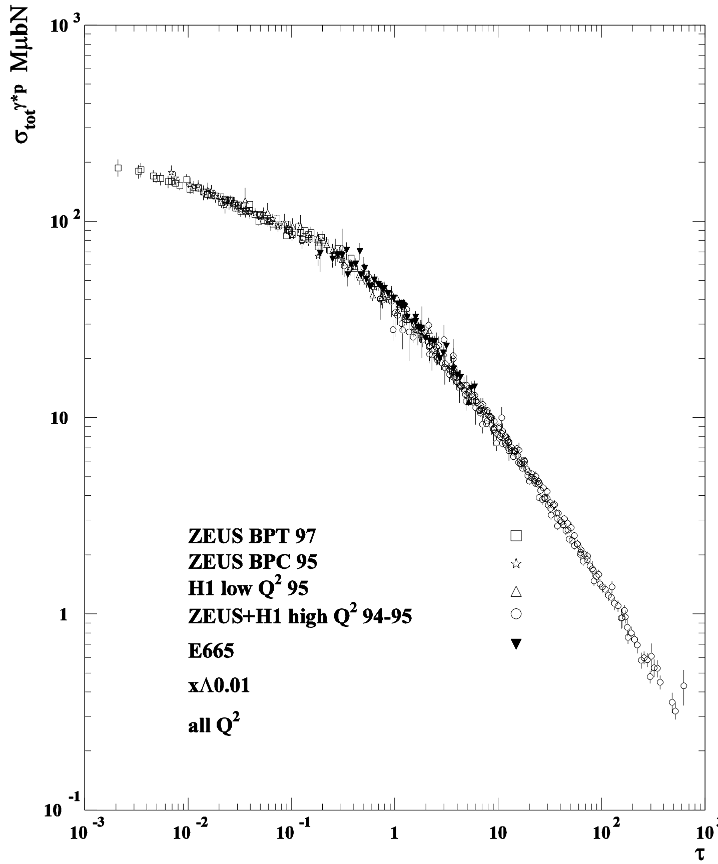

Map of High Energy QCD

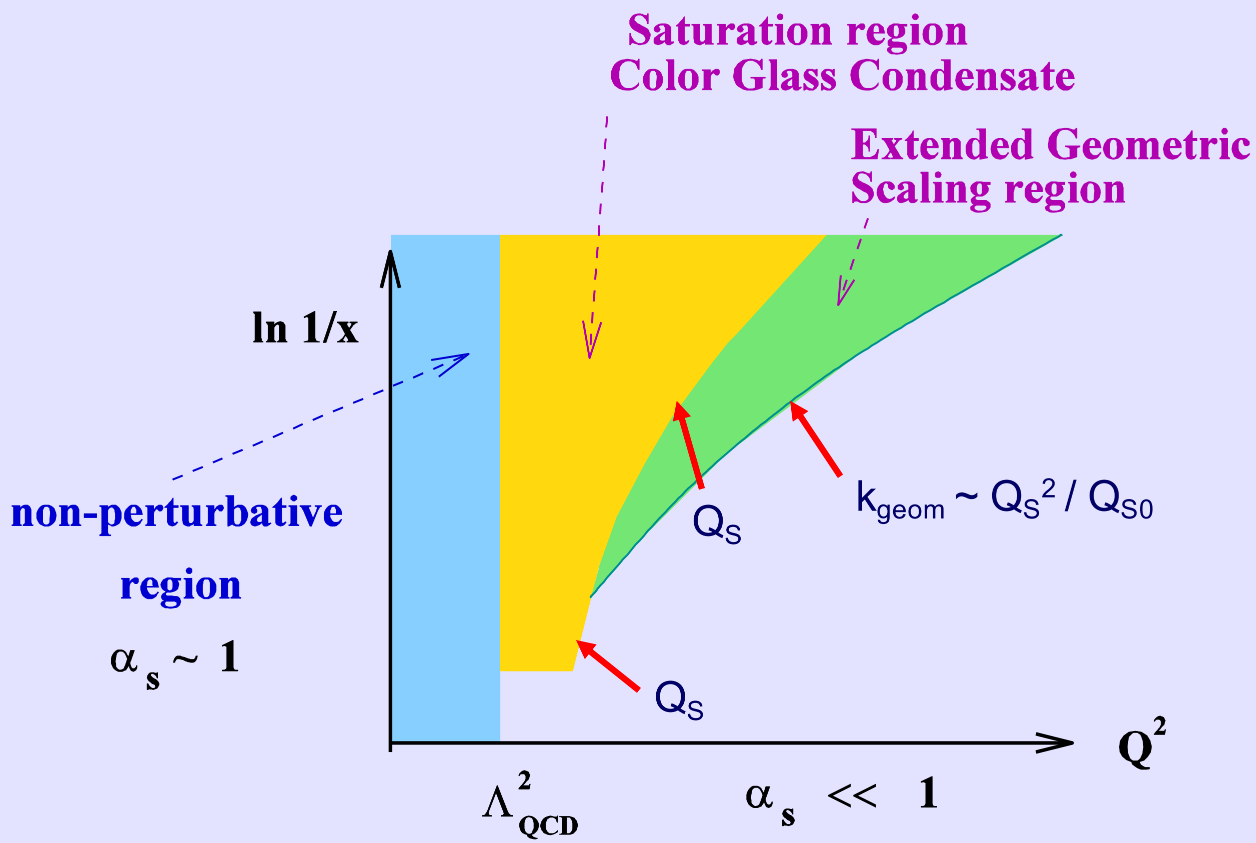

Saturation Scale

To summarize, saturation scale is an increasing function of both energy (1/x) and A:

$$Q_s^2 \sim \left(\frac{A}{x}\right)^{1/3}$$

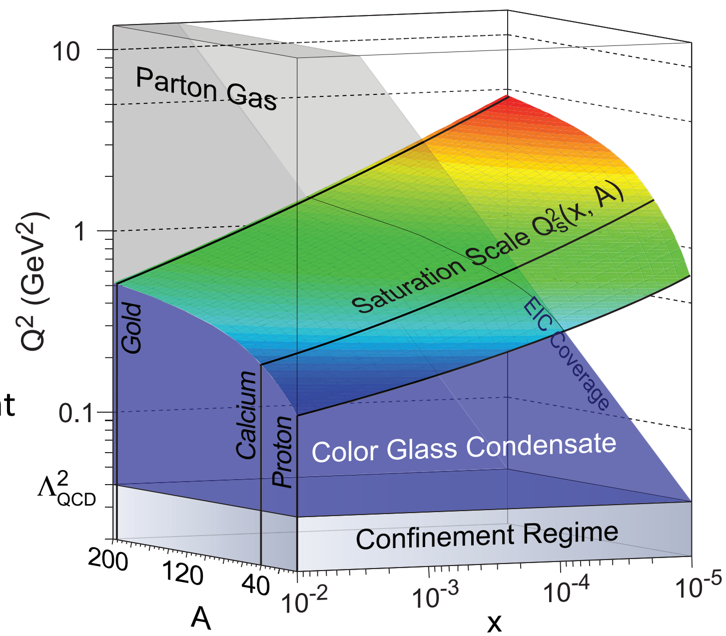

Gold nucleus provides an enhancement by $197^{1/3}$, which is equivalent to doing scattering on a proton at 197 times smaller x / higher s!

References

- E.Iancu, R.Venugopalan, hep-ph/0303204.
- H.Weigert, hep-ph/0501087
- J.Jalilian-Marian, Yu.K., hep-ph/0505052
- F. Gelis et al, arXiv:1002.0333 [hep-ph]
- J.L. Albacete, C. Marquet, arXiv:1401.4866 [hep-ph]
- A. Morreale, F. Salazar, arXiv:2108.08254 [hep-ph]
- and…

References

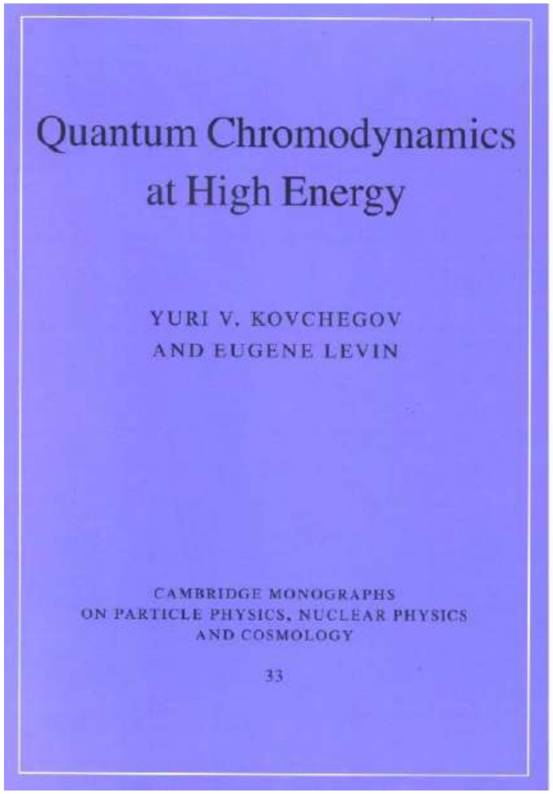

Published in September 2012
by Cambridge U Press

Saturation Physics at EIC

Can Saturation be Discovered at EIC?

EIC will have an unprecedented small-x reach for DIS on large nuclear targets, enabling decisive tests of saturation and non-linear evolution:

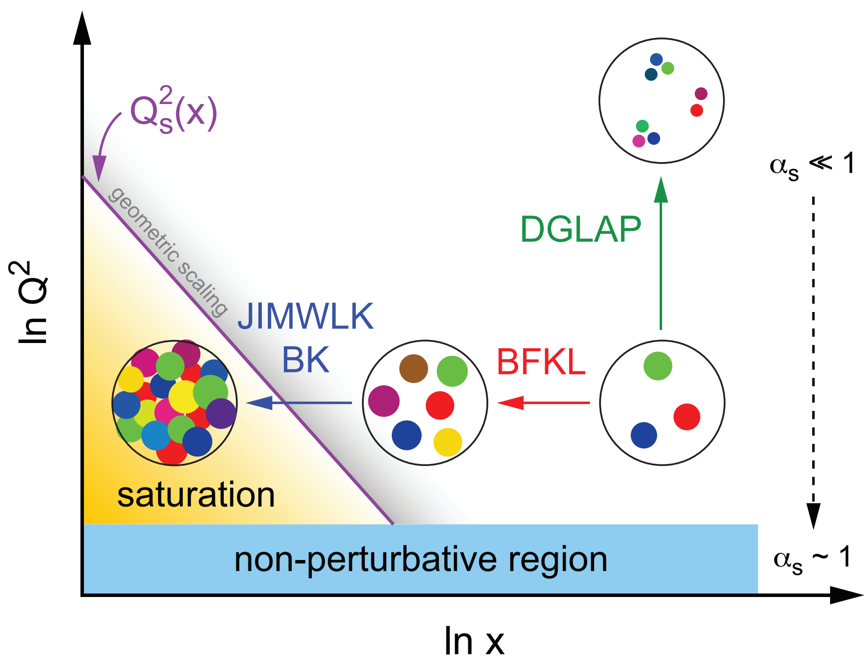

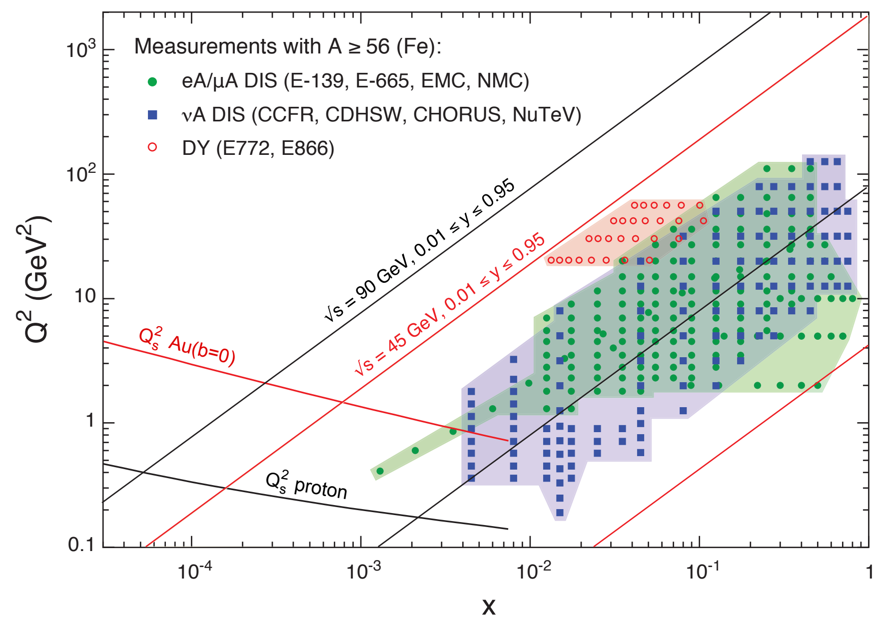

Plots from the EIC White Paper, '12, '14 (2nd ed).

EIC Literature

2002

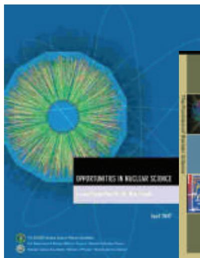

"…essential accelerator and detector R&D [for EIC] should be given very high priority in the short term."

2007

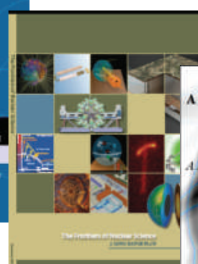

"We recommend the allocation of resources …to lay the foundation for a polarized Eletron-Ion Collider…"

2009

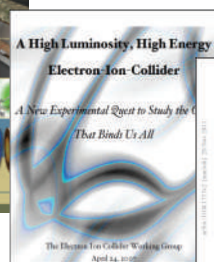

"..a new dedicated facility will be essential for answering some of the most central questions."

2010

"The quantitative study of matter in this new regime [where abundant gluons dominate] requires a new experimental facility: an Electron Ion Collider.."

2012

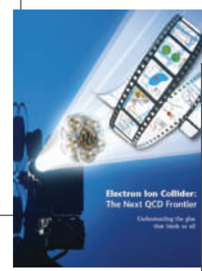

"…essential accelerator and detector R&D [for EIC] should be given very high priority in the short term."

2013

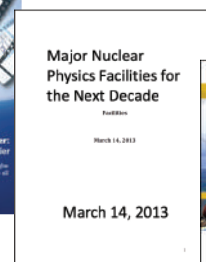

"Electron-Ion Collider..absolutely central to the nuclear science program of the next decade."

"a high-energy high-luminosity polarized EIC [is] the highest priority for new facility construction following the completion of FRIB."

2015

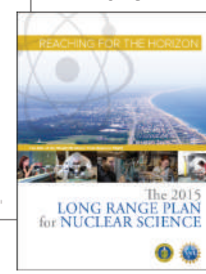

The science questions that an EIC will answer are central to completing an understanding of atoms as well as being integral to the agenda of nuclear physics today."

2018

+ EIC Yellow Report, 2021

Electron-Ion Collider (EIC) White Paper

- EIC WP was finished in late 2012 + 2nd edition in 2014
- A several-year effort by a 19-member committee + 58 co-authors
- arXiv:1212.1701 [nucl-ex]
- We will follow the physics discussion and use the plots from this WP.

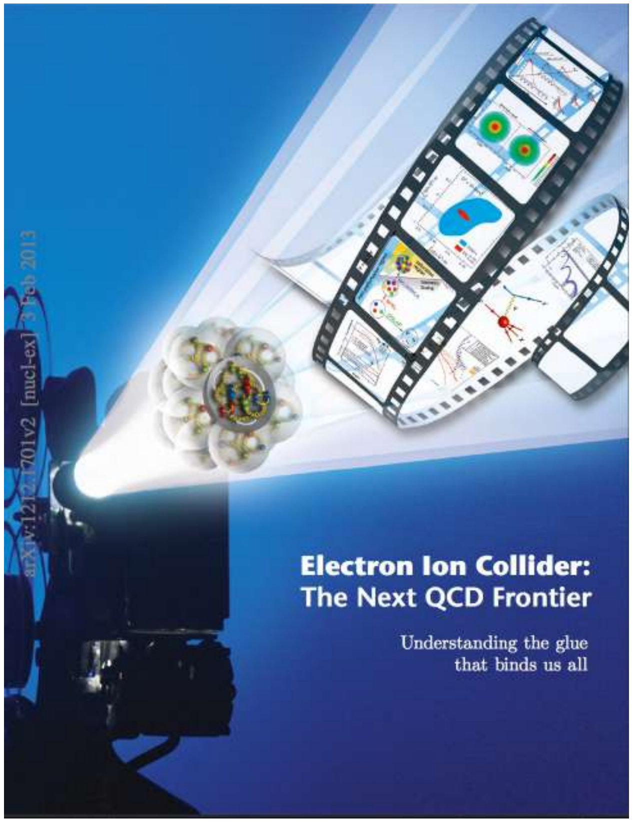

(i) Nuclear Structure Functions

Structure Functions at EIC

Nuclear structure functions F_2 and F_L (parts of σ^{e+A} cross section) which will be measured at EIC (values = EPS09+PYTHIA). Shaded area = (x, Q^2) range of the world e+A data.

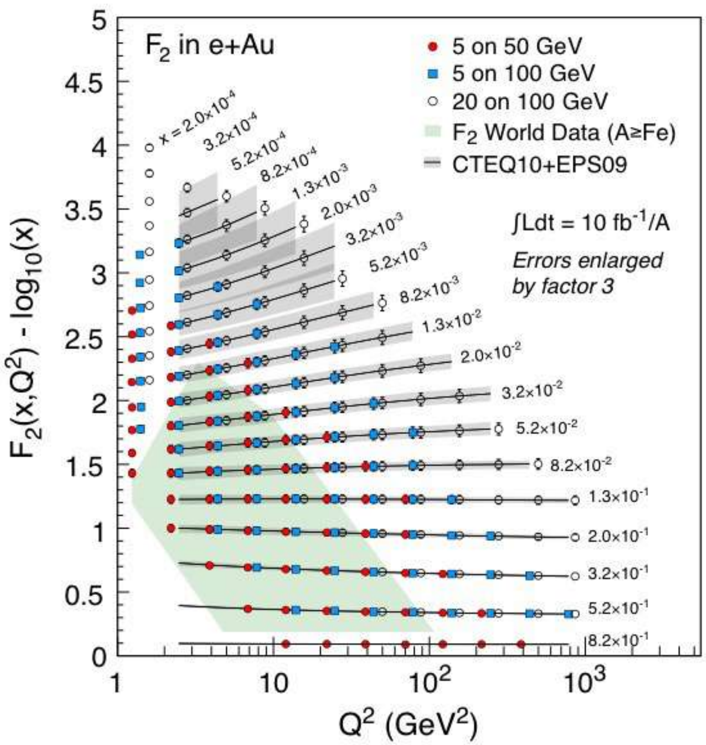

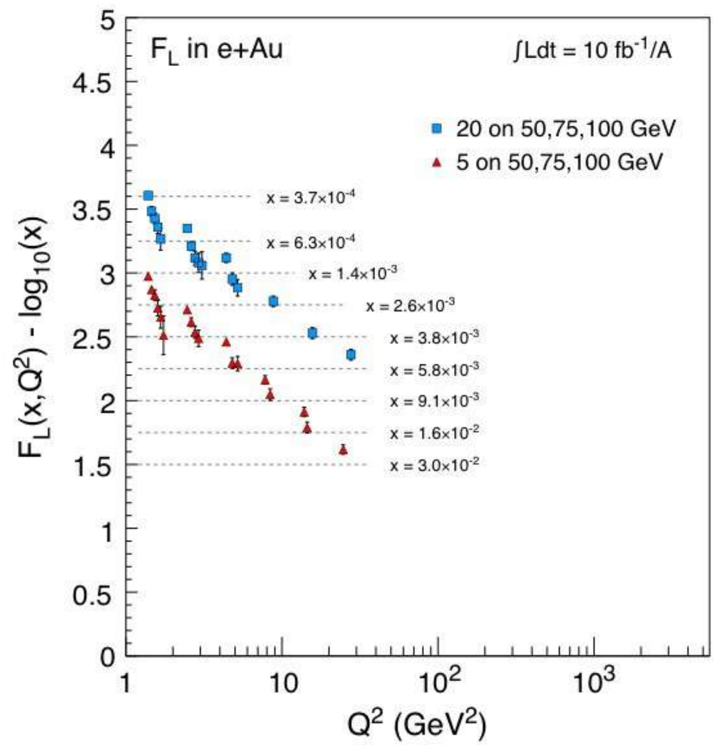

Nuclear Shadowing

- Saturation effects may explain nuclear shadowing: reduction of the number of gluons per nucleon with decreasing x and/or increasing A:

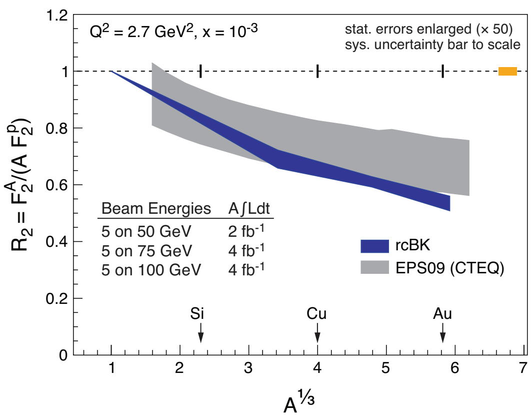

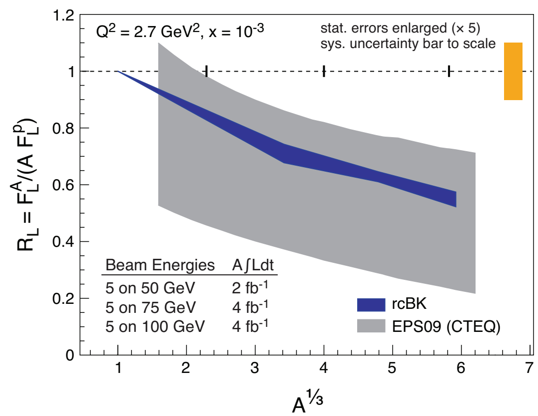

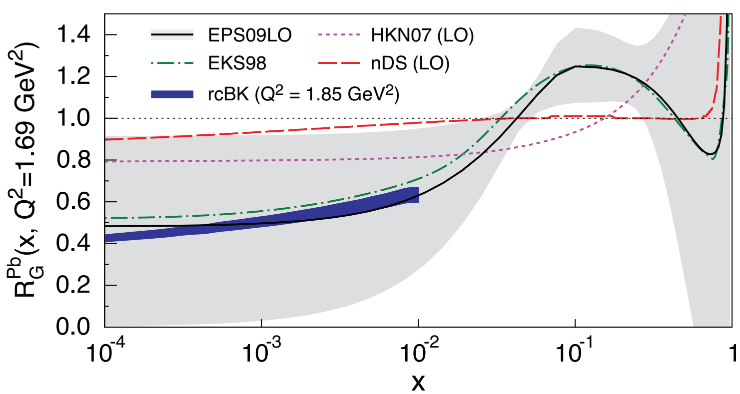

But: as DGLAP does not predict the x- and A-dependences, it needs to be constrained by the data.

Note that including heavy flavors (charm) for F_2 and F_L should help distinguish between the saturation versus non-saturation predictions.

Nuclear Shadowing for Charm

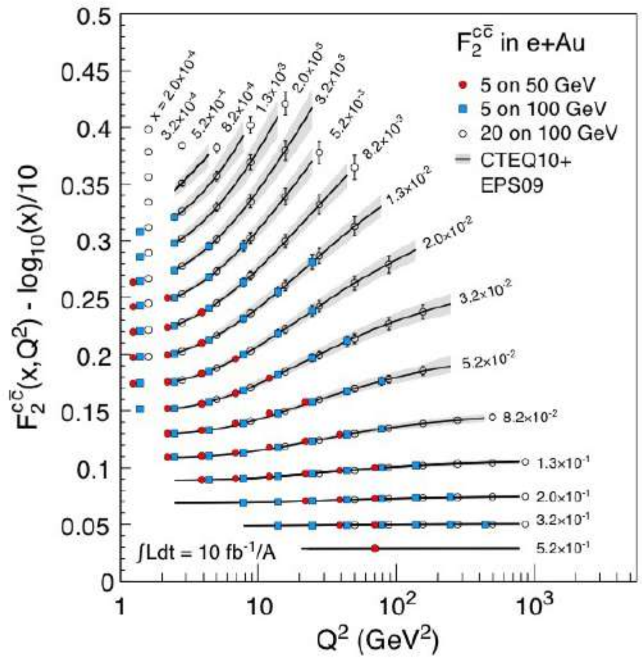

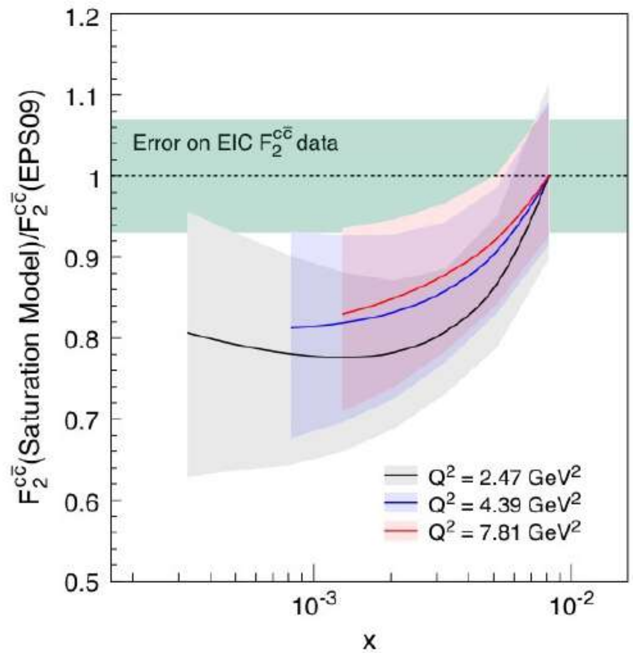

may help distinguish saturation vs DGLAP-based prediction

(ii) Di-Hadron Correlations

De-correlation

- Small-x evolution ↔ multiple emissions
- Multiple emissions → de-correlation.

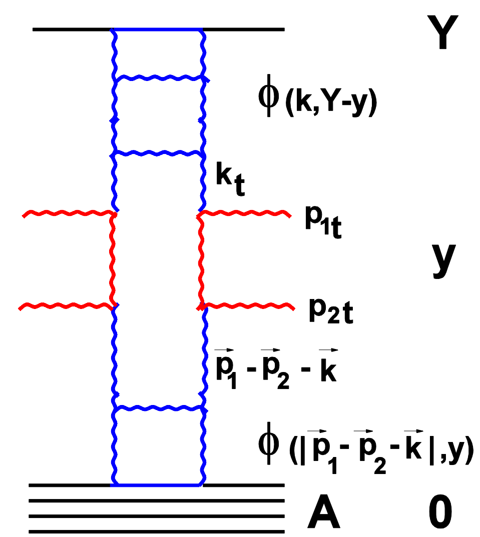

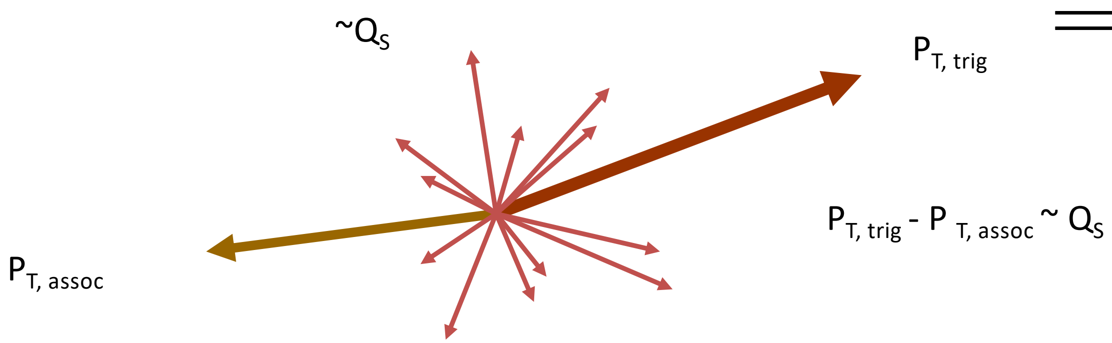

- B2B jets may get de-correlated in p_T with the spread of the order of Q_S

Di-hadron Correlations

Depletion of di-hadron correlations is predicted for e+A as compared to e+p. (Dominguez et al ‘11; Zheng et al ‘14). This is a signal of saturation.

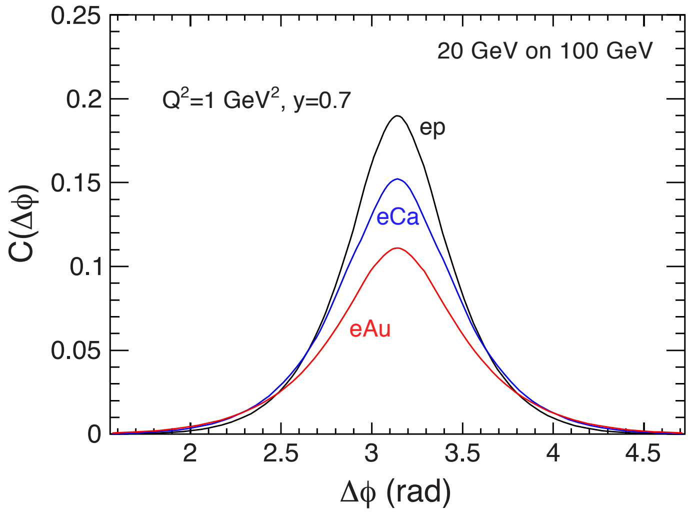

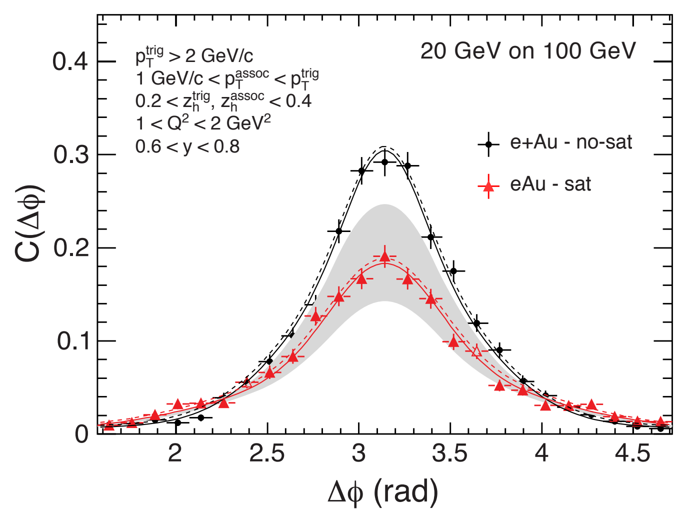

(iii) Diffraction

Diffraction in optics

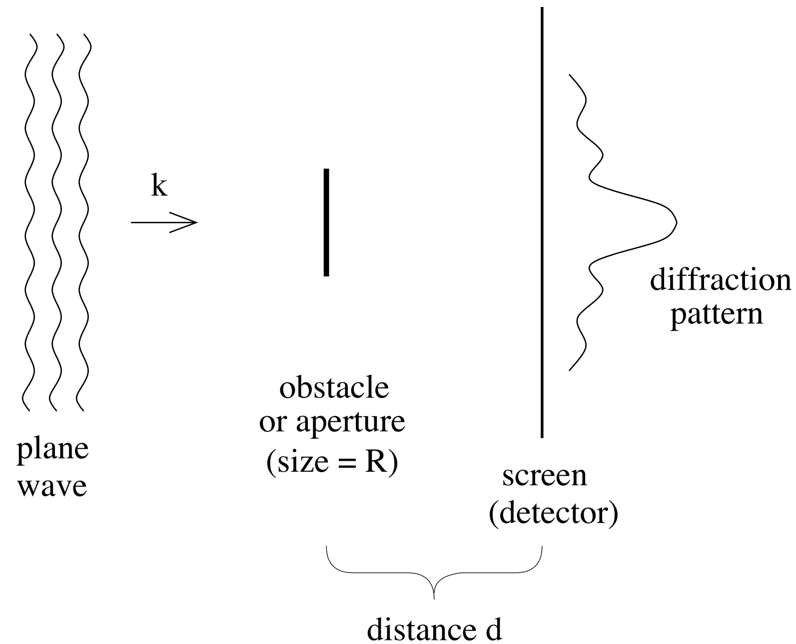

Diffraction pattern contains information about the size *R* of the obstacle and about the optical "blackness" of the obstacle.
In optics, diffraction pattern is studied as a function of the angle θ. In high energy scattering the diffractive cross sections are plotted as a function of the Mandelstam variable *t* with $\sqrt{|t|} = k \sin\theta$.

Optical Analogy

Diffraction in high energy scattering is not very different from diffraction in optics: both have diffractive maxima and minima:

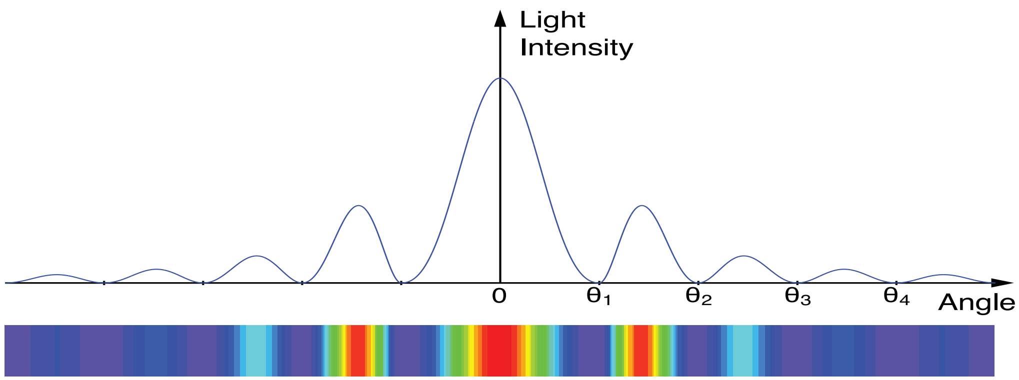

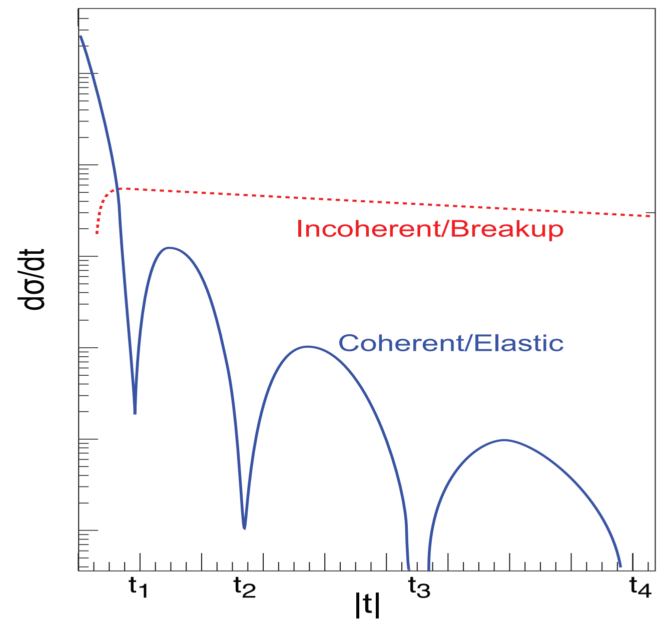

Coherent: target stays intact;
Incoherent: target nucleus breaks up, but nucleons are intact.

Diffraction terminology

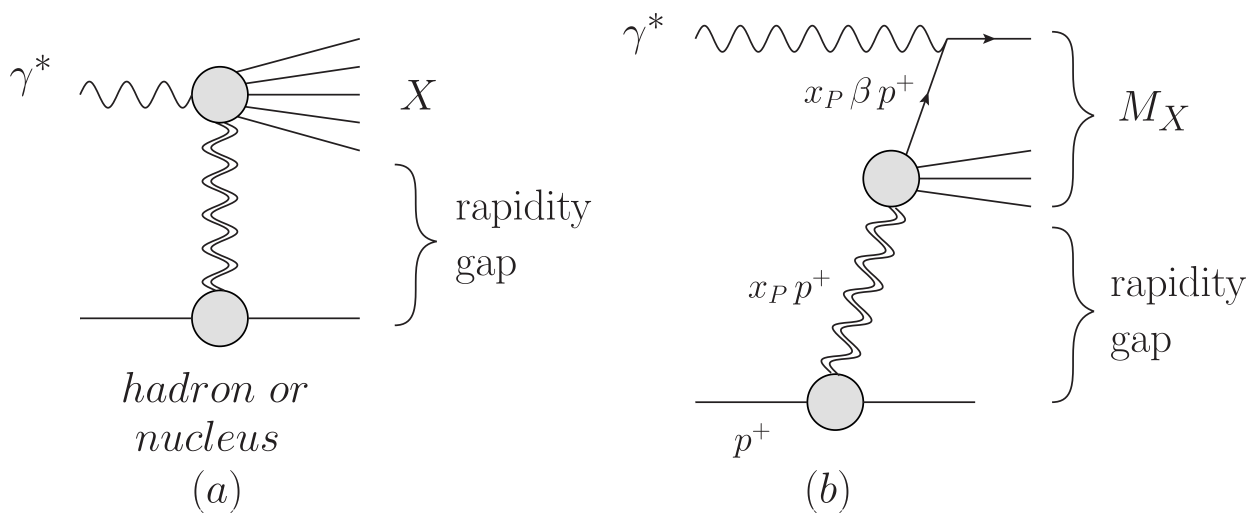

W^2 = cms energy squared
for the photon+proton/nucleus
system

$$x_P = \frac{Q^2 + M_X^2}{Q^2 + W^2} \approx \frac{M_X^2}{W^2} \qquad \beta = \frac{x_{Bj}}{x_P} = \frac{Q^2}{Q^2 + M_X^2} \approx \frac{Q^2}{M_X^2}$$

Quasi-elastic DIS

Consider the case when nothing but the quark-antiquark pair, i.e., two jets, are produced:

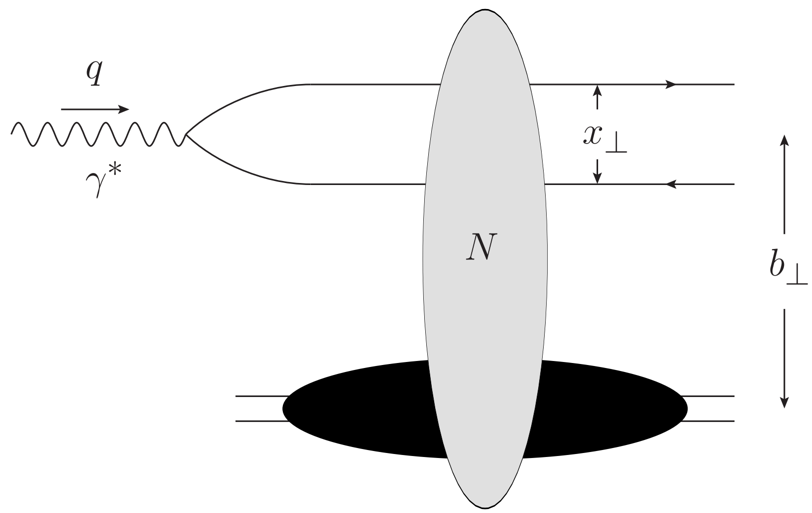

The quasi-elastic cross section is then proportional to the square of the dipole amplitude N:

$$\sigma_{el}^{\gamma^* A} = \int \frac{d^2 x_\perp}{4\,\pi}\, d^2 b_\perp \int\limits_0^1 \frac{dz}{z\,(1-z)}\ |\Psi^{\gamma^* \to q\bar{q}}(\vec{x}_\perp, z)|^2\ N^2(\vec{x}_\perp, \vec{b}_\perp, Y)$$

Buchmuller et al '97, McLerran and Yu.K. '99

Diffraction on a black disk

- For low Q^2 (large dipole sizes) the black disk limit is reached with N=1
- Diffraction (elastic scattering) becomes a half of the total cross section

$$\frac{\sigma_{el}^{q\bar{q}A}}{\sigma_{tot}^{q\bar{q}A}} = \frac{\int d^2b\, N^2}{2\int d^2b\, N} \longrightarrow \frac{1}{2}$$

- Large fraction of diffractive events in DIS is a signature of reaching the black disk limit!
- HERA: ~15% (unexpected!) ; EIC: ~25% expected from saturation

Diffractive over total cross sections

- Here's an EIC measurement which may distinguish saturation from non-saturation approaches (from the 2012 EIC White Paper), using **diffractive to total double ratio**:

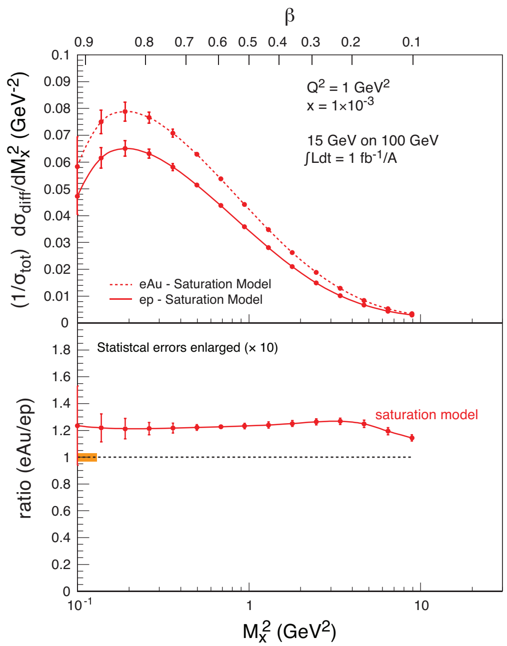

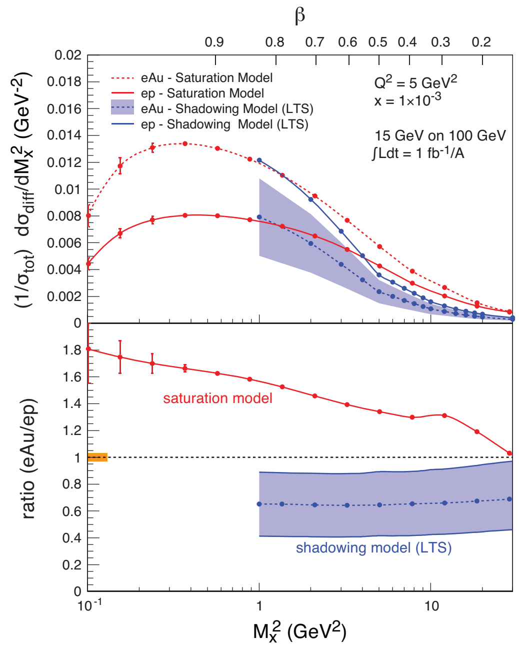

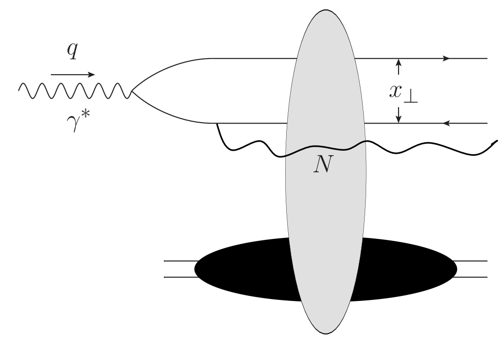

sat = Kowalski et al '08, plots generated by Marquet

no-sat = Leading Twist Shadowing (LTS), Kopeliovich, Tarasov, '02; Frankfurt, Guzey, Strikman '04, plots by Guzey

Exclusive Vector Meson Production

- An important diffractive process which can be measured at EIC is exclusive vector meson production (cf. UPCs):

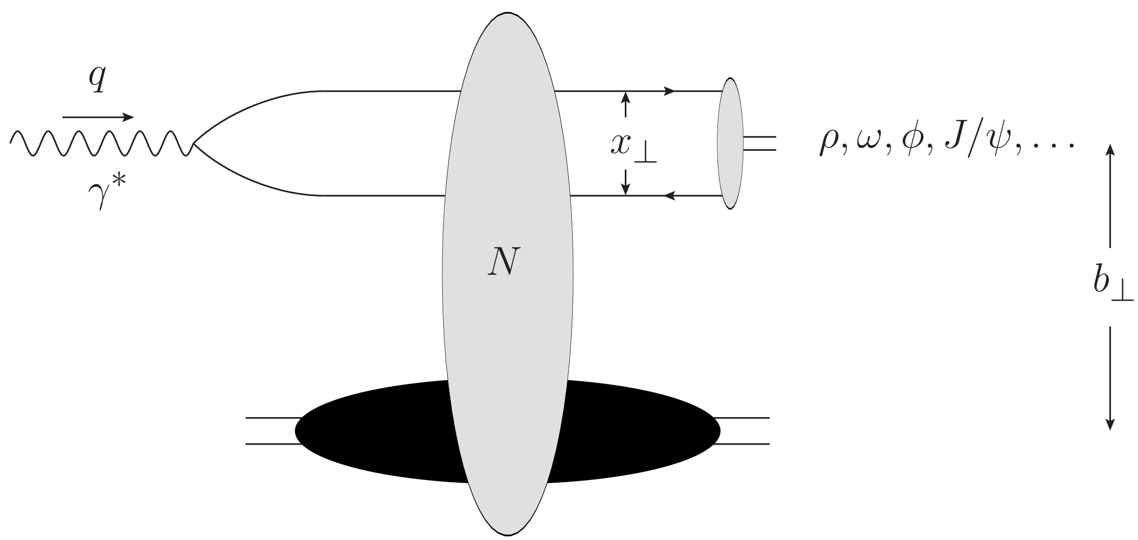

Exclusive VM Production:
Probe of Spatial Gluon Distribution

- Differential exclusive VM production cross section is

$$\frac{d\sigma^{\gamma^*+A\to V+A}}{dt} = \frac{1}{4\pi}\left|\int d^2b\, e^{-i\,\vec{q}_\perp\cdot\vec{b}_\perp}\, T^{q\bar{q}A}(\hat{s},\vec{b}_\perp)\right|^2$$

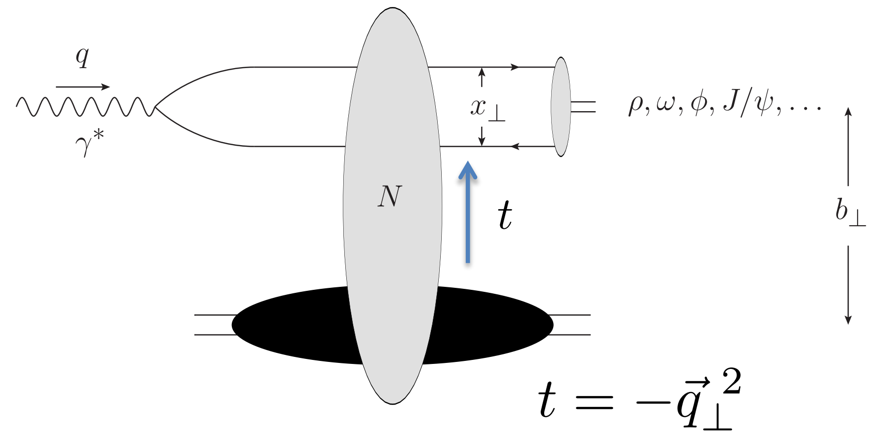

- the T-matrix is related to the dipole amplitude N:

$$T^{q\bar{q}A}(\hat{s},\vec{b}_\perp) = i\int\frac{d^2x_\perp}{4\,\pi}\int_0^1\frac{dz}{z\,(1-z)}\;\Psi^{\gamma^*\to q\bar{q}}(\vec{x}_\perp,z)\;N(\vec{x}_\perp,\vec{b}_\perp,Y)\,\Psi^V(\vec{x}_\perp,z)^*$$

Brodsky et al ‘94, Ryskin ‘93

- Can study *t*-dependence of the *d*σ*/dt* and look at different mesons to find the dipole amplitude *N(x,b,Y)* (Munier, Stasto, Mueller ’01).
- Learn about the gluon distribution in space. This is similar to GPDs.

Exclusive VM Production as a Probe of Saturation

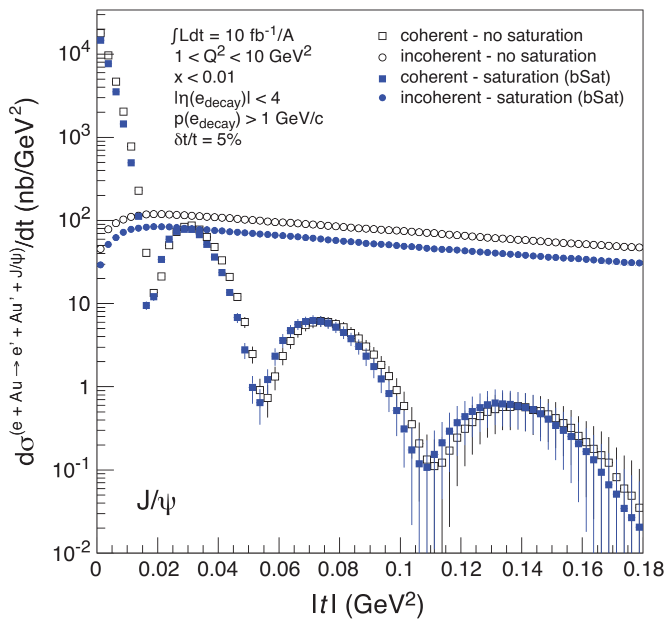

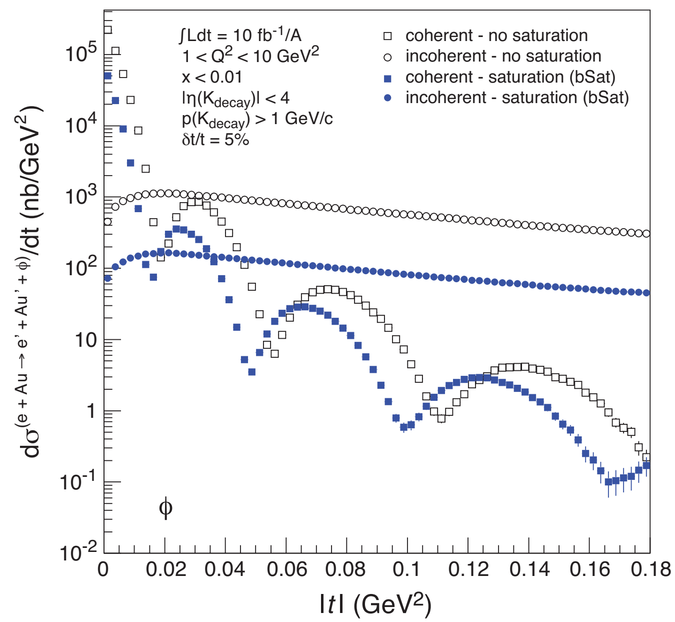

Plots by T. Toll and T. Ullrich using the Sartre event generator
(b-Sat (=GBW+b-dep+DGLAP) + WS + MC, from the 2012 EIC White Paper).

- J/psi is smaller, less sensitive to saturation effects
- Phi meson is larger, more sensitive to saturation effects

Summary

- We have constructed nuclear/hadronic wave function in the quasi-classical approximation (MV model) and studied DIS in the same approximation.
- We included small-*x* evolution corrections into the DIS process, obtaining nonlinear BK/JIMWLK evolution equations.
- Nonlinear evolution restores unitarity at high energies, which was violated by the BFKL equation.
- We found the saturation scale which is large at small x and for large nuclei, justifying the whole procedure.

$$Q_S^2 \sim A^{1/3} \left(\frac{1}{x}\right)^{\lambda}$$

- Saturation/CGC physics predicts geometric scaling observed experimentally at HERA.
- We hope to discover saturation physics at the EIC.